PHOTODEGRADATION OF α-NUCLEATED POLYPROPYLENE

Bc. LEOŠ VAŠEK

Master Thesis
2008

Tomas Bata University in Zlín
Faculty of Technology

Univerzita Tomáše Bati ve Zlíně
Fakulta technologická
Ústav inženýrství polymerů
akademický rok: 2007/2008

ZADÁNÍ DIPLOMOVÉ PRÁCE
(PROJEKTU, UMĚLECKÉHO DÍLA, UMĚLECKÉHO VÝKONU)

Jméno a příjmení:	**Bc. Leoš VAŠEK**
Studijní program:	**N 2808 Chemie a technologie materiálů**
Studijní obor:	**Inženýrství polymerů**
Téma práce:	**Photodegradation of alpha-Nucleated Polylpropylene**

Zásady pro vypracování:

The aim of this Master thesis is to study the effect of α-nucleating/clarifying agent on the photodegradation of polypropylene. Polypropylenes with different amounts of commercial α-nucleating agent Millad 3988 based on 1,3;2,4-bis(3,4-dimethylbenzylidene)sorbitol will be UV-irradiated and then examined by several methods. Infrared spectroscopy, X-ray scattering, differential scanning calorimetry and optical microscopy will be employed.

Rozsah práce:

Rozsah příloh:

Forma zpracování diplomové práce: **tištěná/elektronická**

Seznam odborné literatury:

1. **Wypych, G.: Handbook of Material Weathering (2nd Edition), ChemTec Publishing, 1995, ISBN: 1-895198-12-7**
2. **Wypych, G.: Weathering of Plastics - Testing to Mirror Real Life Performance, Wiliam Andrew Publishing/Plastics Design Library, 1999, ISBN: 1-884207-75-8**
3. **Karger-Kocsis, J.: Polypropylene - An A-Z Reference, Springer - Verlag, 1999, ISBN: 0-412-80200-7**
4. **Maier, C.; Calafut, T.: Polypropylene - The Definitive User's Guide and Databook, Wiliam Andrew Publishing/Plastics Design Library, 1998, ISBN: 1-884207-58-8**

Vedoucí diplomové práce: **Ing. Jana Navrátilová**
Ústav inženýrství polymerů

Datum zadání diplomové práce: **11. února 2008**

Termín odevzdání diplomové práce: **16. května 2008**

Ve Zlíně dne 11. února 2008

doc. Ing. Petr Hlaváček, CSc.
děkan

L.S.

Ing. Roman Čermák, Ph.D.
ředitel ústavu

ABSTRACT

The aim of this Master thesis is to study the effect of α-nucleating/clarifying agent on photodegradation of polypropylene. Samples of polypropylene with different amounts of commercial α-nucleating agent Millad 3988 based on 1,3;2,4-bis(3,4-dimethylbenzylidene)sorbitol were exposed to the UV-radiation for several exposition durations and then examined by several methods. The changes in the samples were monitored by infrared spectroscopy, X-ray scattering, differential scanning calorimetry and optical microscopy. It was found that α-nucleating agent Millad 3988 does not significantly influence the extent of photooxidation. However, it affects the course of oxidation, mainly the formation of the cracks on the surface of the samples.

ANOTACE

Cílem této diplomové práce je studium vlivu α-nukleačního činidla na fotodegradaci polypropylenu. Vzorky polypropylenu s různým obsahem α-nukleačního činidla Millad 3988 na bázi 1,3;2,4-bis(3,4-dimethylbenzyliden)sorbitolu byly vystaveny UV záření v různých časových intervalech a následně zkoumány různými metodami. Změny, které se vyskytly ve vzorcích, byly sledovány infračervenou spektroskopií, rentgenovou difrakcí, diferenciální skenovací kalorimetrií a optickou mikroskopií. Bylo zjištěno, že použití α-nukleačního činidla Millad 3988 nemá zásadní vliv na rozsah fotooxidace. Ovlivňuje však průběh oxidace, a to zejména vznik trhlin na povrchu vzorků.

ACKNOWLEDGEMENTS

In the first place I would like to thank my supervisor Jana Navrátilová for her help in the course of full time of my work.

In the second place I would like to thank my girlfriend Lucie Pšenčíková, my mother Dagmar Vašková and my grandfather Jan Sedláček for kind support during my studies and making this thesis.

I declare I worked on this Bachelor thesis by myself and I have mentioned all the used literature. In the case of publication of results I will noted as co-author.

Zlín, __.__.2008 _____

jméno

TABLE OF CONTENTS

INTRODUCTION

Polymers are relatively new class of materials. They have been developed to take place of some natural materials for their specific properties. Initially the polymers were produced without the exhaustive knowledge of their properties. The result was the financial loss, which inspired distrust to this material. One of the causes of ineffectual applications of polymeric materials was the bad knowledge of their resistance in their surrounding environment. The plastics are not suitable for the universal use. The applicability depends on their chemical composition, structure, the amount and the composition of the fillers, impurities and admixtures. The way of processing, chemical composition and specifications of the environment have to be also considered.

This Master thesis is addressed to photodegradation of α-nucleated polypropylene. Polypropylene belongs to the group of polyolefins, which represent quantitatively the greatest group of synthetic polymers. Isotactic polypropylene (iPP) is one of the most important semicrystalline polymers. This polymer exhibits excellent chemical resistance, low density, relatively high tensile strength and high melting point. Polypropylene is called as polymorphic material. By using varied preparation procedures iPP exhibits four morphological forms on the crystal lattice: α (monoclinic), β (trigonal), γ (orthorhombic) and smectic.

Isotactic polypropylene is frequently used for outdoor applications. However, the sunlight radiation, with connection with other weather conditions like temperature or humidity, strongly influences durability of polypropylene and its useful properties. The loss of these properties is the reason of lifetime decrease of polypropylene products. Therefore, the study of degradation and possibilities of its retardation are on a main interest.

Specific nucleation of PP by α-nucleating agent is used to reduce processing times or to improve properties of polypropylene, especially its transparency. The α-nucleation of PP is described in many papers [e. g. 1, 2]. It has been found that the commercial α-nucleating agent Millad 3988 which is used in this study, is sensitive to thermal degradation [3]. On

the other hand, nearly no interest is focused on the effect of Millad 3988 on photooxidative degradation of polypropylene [4].

The aim of this Master thesis is to study the effect of α-nucleating/clarifying agent on photodegradation of polypropylene. This work compares and describes the process of fotodegradation of iPP samples with different amounts of commercial α-nucleating agent Millad 3988. The specimens were prepared via compression moulding and subsequently, the specimens were exposed to UV-light in accelerated ageing device. The extent of photooxidation was measured using infrared spectroscopy, X-ray scattering, differential scanning calorimetry and optical microscopy.

I. THEORETICAL PART

1 POLYPROPYLENE

Polypropylene is one of the most often used synthetic polymers, especially due to its good availability and low price. The worldwide consumption of polypropylene occupies third place among commodity plastics, after low-density polyethylene and polyvinylchloride but before high-density polyethylene and polystyrene [5].

Moreover, polypropylene is very well processed by various technological processes and it has useful properties. It is a linear hydrocarbon polyolefin or saturated polymer. This material was introduced to the large scale production in 1957 as a plastic and fibre forming material [6].

1.1 Polymerization

As early as 1869 propylene was polymerized by Berthelot by reaction with concentrated sulphuric acid. The resulting viscous oil, at room temperature, did not exhibit interesting properties for industrial application. Its industrial importance results from the appearance of crystalline high molecular weight polypropylene, which was first polymerized in 1955 by Natta from organo-metallic catalysts based on titanium and aluminium (Fig. 1.1). The resulting semi-crystalline polymer has strong mechanical properties which explain its rapid industrial development.

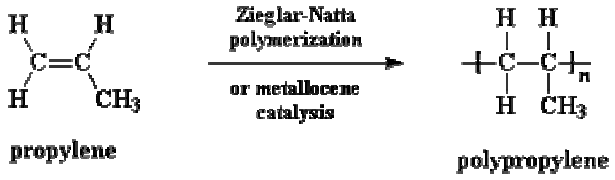

Fig. 1.1: Polymerization of propylene [7]

The monomer for PP production is obtained by the cracking of petroleum products, such as natural gas or light oils. For the preparation of polypropylene the C_3 fraction (propylene and propane) is the basic intermediate and it can be separated from the other gases without undue difficulty by fractional distillation. Polypropylene is then prepared

using Ziegler-type catalysts or metallocene catalysts by a polymerization. A typical catalyst system may be prepared by reacting titanium trichloride with aluminium triethyl, aluminium tributyl or aluminium diethyl monochloride in naphtha under nitrogen to form slurry consisting of about 10 % catalyst and 90 % naphtha. The properties of the polymer are strongly dependent on the catalyst composition and its particle shape and size [8].

1.2 Structure

Polymerization of the non-symmetrical propylene molecule leads to three possible sequences: head-to-head, head-to-tail and tail-to-tail. The steric effect of the methyl group highly favours the head-to-tail sequence, which gives a high chemical regularity of the PP chain [9].

Three stereo-configurations of polypropylene are known: isotactic, syndiotactic and atactic (Fig. 1.2).

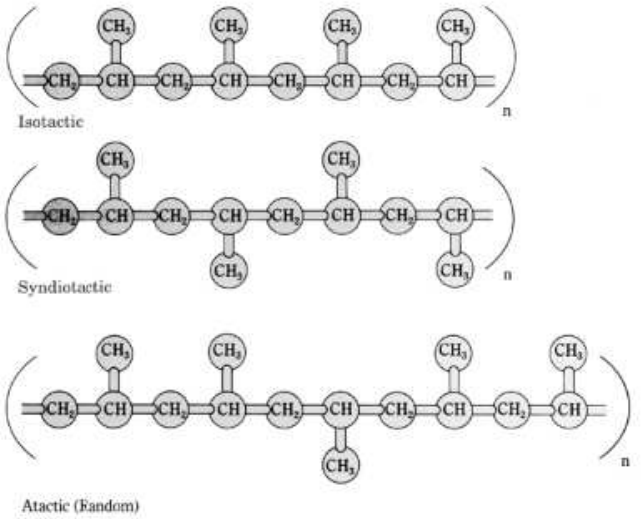

Fig. 1.2: Stereo-configurations of propylene sequences: a) isotactic; b) syndiotactic; c) atactic [10]

1.2.1 Isotactic polypropylene

In isotactic polypropylene (iPP), the most common commercial form, pendant methyl groups are all in the same configuration and are on the same side of the polymer chain [10].

Due to its tacticity, iPP is the most stereo-regular structured polypropylene when compared to atactic and syndiotactic polypropylene and thus higher degree of crystallinity (60−70 %) is involved. Increased crystallinity of PP results in good mechanical properties such as stiffness and tensile strength. This allows polypropylene to be used as a replacement for engineered thermoplastics, such as ABS [12].

Molecules of polypropylene cannot crystallize in a planar zigzag form because of the steric hindrance of the methyl group, but crystallize in a helix, with three molecules being required for one turn of the helix [8]. The helix can be either right- or left-handed, with a periodicity of 0.65 nm. The position of the methyl group with respect to the chain axis can be either up or down [11].

1.2.2 Syndiotactic polypropylene

Syndiotactic polypropylene (sPP) is defined by methyl groups arranged alternatively on both side of the zigzag chain, and it is obtained by alternative addition of the two stereoisomeric configuration form of propylene monomer. In the early 1990s syndiotactic polypropylene became available from a number of sources and were joined in the late 1990s by Dow using metallocene catalyst systems [8, 9].

Sequence for each syndiotactic unit sets up a helix with two syndiotactic units per turn with a period of 0.74 nm. The stable structure of sPP has a unit cell which includes two left- and two right-handed helices in a regular alternation along both the *a* and the *b* axis. In real crystals the regular left-right packing is often dislocated, leading to lattice disorder. This disorder is known to increase with decreasing crystallization temperature (T_c). Syndiotactic polypropylene forms both hedrites and spherulites, depending on the T_c. Going to lower T_c, an increasing tendency of branching and splaying of growing lamellae continuously changes the hedrites into spherulites [14].

Interest in this material is a consequence of its possessing greater toughness, clarity and heat resistance (softening point) than corresponding isotactic polypropylene [8].
Syndiotactic polypropylene finally found the application in adhesives, caulks, and cable-filling compounds [7].

1.2.3 Atactic polypropylene

Atactic or amorphous polypropylene (aPP) is characterized by a random steric orientation of the methyl pendant groups on the tertiary carbon atoms along the molecular chain. The random sequence of these methyl substituents is linked to an atactic configuration. Due to its fully amorphous nature, aPP is easy soluble (even at ambient temperatures) in a great number of aliphatic and aromatic hydrocarbons, esters and other solvents in contrast to the isotactic PP of semicrystalline feature [13].

Generally atactic polymers are characterized by their tacky, amorphous behaviour and low molecular weights. Atactic portion provide the same effect as a plasticizer, by reducing the crystallinity of the polypropylene. A small amount of atactic polymers in the final polymer can be used to improve certain mechanical properties. This provides properties to the final polymer, such as improved low temperature performance, elongation, processability and optical properties (transparency), but sacrifices flexural modulus or stiffness, and long-term heat ageing properties [7].

Most polymers are predominantly isotactic, with small amounts of atactic polymer. New metallocene catalysts make possible other stereochemical configurations, such as hemiisotactic polypropylene. In this configuration, the most pendants methyl groups are on the same side of the polypropylene chain, as in isotactic polypropylene; however, other methyl groups are inserted at regular intervals on the opposite side of the chain [10].

1.3 Morphology

On the crystal lattice level, iPP exhibits three different morphological forms: α (monoclinic), β (trigonal) and γ (orthorhombic), distinguished by the arrangement of the chains. Another form of iPP with a degree of order between crystalline and amorphous phases is a smectic form. Preparation of these forms depends on the crystallization conditions, such as pressure, temperature, cooling rate and addition of nucleating agents [10, 11].

1.3.1 α-form

The predominant crystal structure of pure isotactic polypropylene at atmospheric pressure is the monoclinic α-structure. The equilibrium melting temperature of the α-form of iPP crystals (T_m^0) was reported between 185 °C and 209 °C [11, 15]. Turner-Jones et al. calculated the parameters of a unit cell, which contains four three-fold helical chains, and found: a = 0.666 nm, b = 2.078 nm, c = 0.6495 nm, β = 99.62 ° and α = γ = 90 °. The number of repeating units involved in each unit cell is twelve, and the crystallographic density is 0.946 g.cm^{-3} [16]. A model of α-form crystal structure is schemed in Fig. 1.3.1.

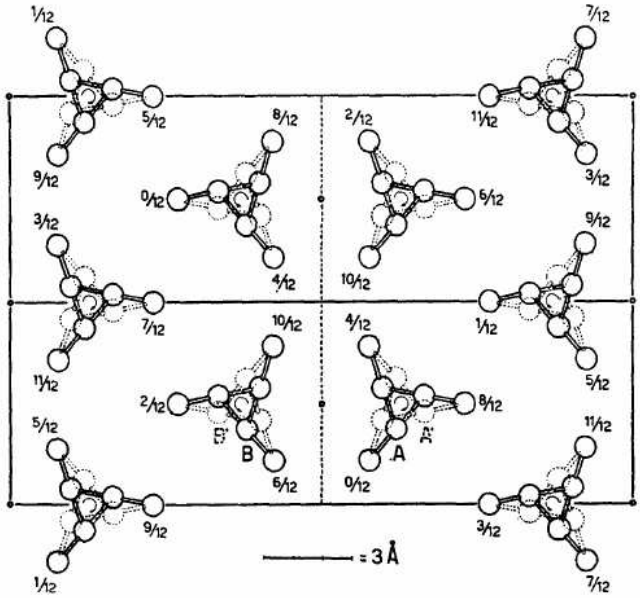

Fig. 1.3.1: Crystal structure of α-phase of iPP [13]

Polymer chains in the α-phase form a helical structure in a monoclinic unit cell, and fold into lamellae with thicknesses of 5–20 nm. Radial growth of lamellae is dominant; however, lamellae can also associate tangentially, with the tangential lamella branching off approximately orthogonally from the plane of the radial lamellae. This forms a cross-hatched structure in the lamellae, which aggregate to form spherulites [8]. The α-form of iPP exhibits three types of spherulites [11]:

1. Positive birefringence spherulites (α_I) can be developed at an isothermal crystallization temperature below 132 °C;
2. Negative birefringence spherulites (α_{II}) can be prepared at a temperature greater than 138 °C;
3. Mixed birefringence spherulites (α_{III}) can be observed at any temperature up to 150 °C.

The lamellar structure produces positive, negative, and mixed birefringence. Negative birefringence results from spherulites in which radial lamella are dominant, while positive birefringence is due to spherulites with predominantly tangential lamellae. Both negatively and positively birefringent spherulites form a Maltese cross pattern under crossed polarizers. In spherulites with mixed birefringence, neither tangential nor radial lamellae are predominant, and a distinct Maltese cross is not formed. The birefringence changes from positive to negative with increasing crystallization temperature, as the tangential lamellae undergo premelting. The α-phase of isotactic polypropylene is the primary phase of polypropylene obtained under usual processing conditions [8].

1.3.2 β-form

The β-modification of iPP was firstly identified in 1959 by Keith et al. In the crystallization of conventional iPP grades, a small amount of β-modification occurs sporadically at high supercoolings (T_c < 130 °C) or in quenched samples. However, under special crystallization conditions, when the temperature gradient method is used or when selective β-nucleating agents are present a high amount of β-modification is produced (β-iPP i.e. iPP with dominant β-structure). The most widespread high active β-nucleating agent is a γ-quinacridone red pigment. Some two-component compounds obtained by the reactions of certain organic acids with $CaCO_3$, also possess a very high β-nucleating activity. The β-modification of iPP has a trigonal unit cell structure, with more disorder than the α-modification (Fig. 1.3.2) [10, 17].

The parallel, stacked lamella does not show cross-hatching. Lamella has been observed to form sheaf-like spherulitic structures with interconnected boundaries, different from the distinct boundaries of α-modification spherulites. The derivation of the unit cell of the β-modification has been attempted by many researchers; a more satisfactory model of the unit cell is the trigonal, which contains three isochiral helices with a = b = 1.101 nm and c = 0.65 nm, ρ = 0.92 g.cm^{-3} [18].

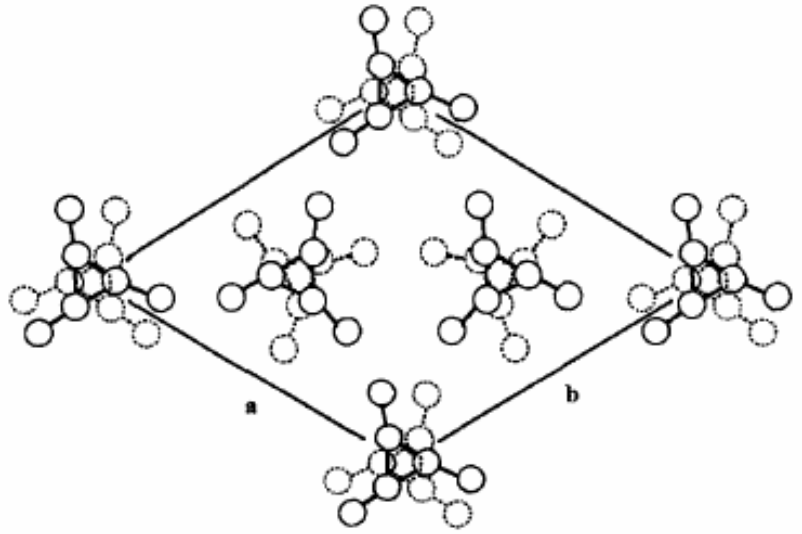

Fig. 1.3.2: Crystal structure of β-phase of iPP [13]

The β-form exhibits negative birefringence under crossed polarizers and can convert to the α-form on slow heating. Two types of β-spherulites were developed [11]:

1. Negative radial β-spherulites, which grow below 128 °C;
2. Negative ringed β-spherulites which are observed between 128 and 135 °C.

Some properties of β-iPP differ significantly from those of α-iPP except glass temperature, which is identical. In comparison with α-iPP, β-iPP possesses lower crystal density, melting temperature and fusion enthalpy. The chemical resistance of β-iPP seems to be lower than of α-iPP. The impact strength and toughness of β-iPP exceed those of α-iPP, but at the other hand, it has a lower elasticity modulus and yield stress than α-iPP [18].

1.3.3 γ-form

This form was discovered in 1961 by Addink & Beintema [19]. It was produced by crystallization at elevated pressures from high molecular weight homopolymer [11]. The γ-form predominates when the pressure during the crystallization is higher than 200 MPa. Other procedure which leads to the growth of this form is crystallization from the melt of high molecular weight stereoblock copolymer with small amounts of ethylene or but-1-ene.

The crystal structure and unit cell geometry of the γ-form in iPP are known only approximately, and bear strong resemblance to those of the α-form. The γ-form was firstly identified as triclinic [15]. By contrast, the cell structure proposed by Brückner et al. has a face-centered orthorhombic unit cell with parameters a = 0.85 nm, b = 0.993 nm and c = 4.241 nm containing isochiral helices (Fig. 1.3.3). It is unique in polymer crystallography: the chain axes in adjacent crystal layers are not parallel. The angle between the chain stems is about 80 ° . The density of γ-form is the same as the density of α-form [11, 13].

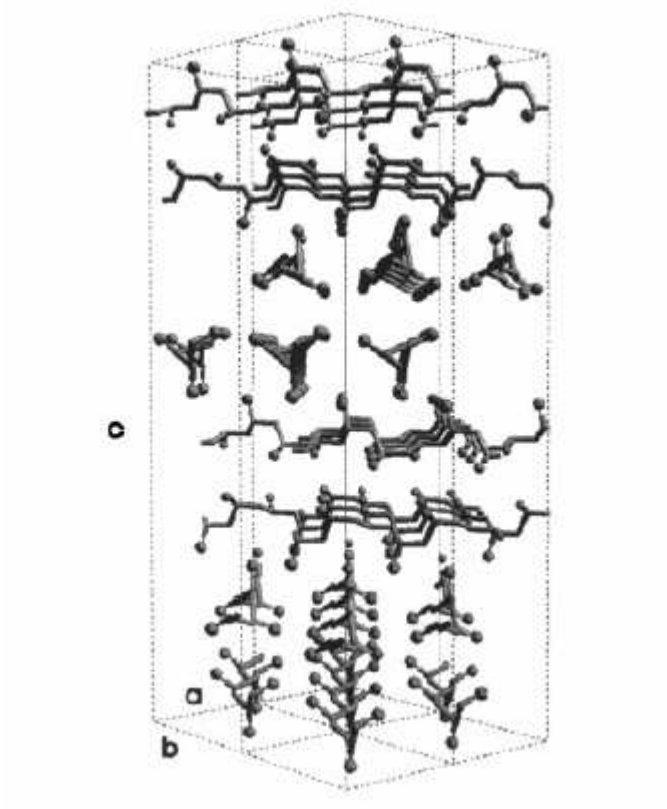

Fig. 1.3.3: Four unit cells of the γ-modification of iPP according to the nonparallel chain packing model of Meille et al. [20]

On the spherulitic level, pure γ-form shows negative birefringence, lathlike structure of the α-form is absent in the γ-spherulites. The melting point of the γ-form is mostly reported in the range of 125 to 150 °C for low molecular weight samples. In the case of

pressure-crystallized samples of high molecular weight iPP, the melting occurs above 150 °C [11].

1.3.4 Smectic form

The mesomorphic or smectic form of polypropylene is a noncrystalline phase, intermediate in order between crystalline and amorphous forms. Early experiments indicated that this form might be a paracrystalline phase resulting from deformed or distorted lattice structures. Examples of lattice defects include atoms forced out of normal lattice or unit cell positions due to surrounding amorphous material, changes in polymer chain folding, presence of atoms of foreign material in the lattice, and screw dislocations that disrupt the spherulite structure by initiating lamellar growth in an irregular location. Polymer chains have been shown to form helical structures, but the unit cell and lamellar structures have not yet been well resolved. Experiments indicate a lack of lamellar order in addition to a low density and small size of ordered structures. These characteristics result in high clarity, useful in quenched film applications [10].

1.4 Properties

Commercial PP is 90–95 % isotactic. The average molecular weights of iPP are in range M_n = 38 000−60 000 g.mol^{-1} and M_w = 220 000−700 000 g.mol^{-1} with a polydispersity of 6–12. The crystalline regions have a density of 0.94 g/cm^3 and the amorphous regions have a density of 0.85 g/cm^3, so that overall, PP has a density about 0.90 g/cm^3 with a crystallinity of about 50 %. PP melts may be quenched to give an amorphous polymer. The maximum melting temperature (T_m) value is 165 °C with narrow (about 5 °C) melting range, so that PP softens at a considerably higher temperature than polyethylene (PE). Its major amorphous transition is at about 0 °C so that the polymer embrittles markedly on cooling [7].

PP is stiffer than PE, having a tensile modulus of 1 000–1 300 MPa and a tensile strength of 25−35 MPa. Its elongation at break is 50–300 % and its impact strength (Izod) is 0.3–4.3 J. Polypropylene is highly solvent resistant and environmental stress cracking resistant. It has very high electrical resistivity. However, the presence of a tertiary carbon

on each repeated unit makes it very susceptible to oxidative degradation. Although usually opaque, thin film, especially if biaxially oriented, may show a sparkling degree of clarity. Unaxially oriented film may be readily split in the direction of orientation to give tape, twine or fibres [7].

Mechanical properties of PP are strongly dependent on its crystallinity. Increasing crystallinity enhances stiffness, yield stress, and flexural strength, however, decreases toughness and impact strength [10]. Some properties of commercial PP are summarized in Table 1.1.

Table 1.1: Some mechanical and thermal properties of commercial polypropylenes

Property	Test method	Homopolymers			Copolymers	
Melt flow index (g/10 min)	(a)	3.0	0.7	0.2	3.0	0.2
Tensile strength (MPa)	(b)	34	30	29	29	25
Elongation at break (%)	(b)	350	115	175	40	240
Flexural modulus (MPa)	□	1 310	1 170	1 100	1 290	1 030
Brittleness temperature (°C)	ICI/ASTM D.476	15	0	0	-15	-20
Vicat softening point (°C)	BS 2782	145-150	148	148	148	147
Rockwell hardness (R-scale)	□	95.0	90.0	90.0	95.0	88.5
Impact strength (J)	(c) 13.5	34.0	46.0	46.0	57.5	□

(a) Standard polyethylene grader: load 2.16 kg at 230 °C

(b) Straining rate 18 in/min

(c) Falling weight test on 14 in diameter moulded bowls at 20 °C

1.5 Applications

Polypropylene has many applications. Injection-molding applications cover a broad range from automotive uses such as dome lights, kick panels, and car battery cases to luggage and washing machine parts. Filled PP can be used in automotive applications such as mounts and engine covers. Elastomer-modified PP is used in the automotive area for bumpers, fascia panels, and radiator grills. Ski boots are another application for these materials. Structural foams, prepared with glass-filled PP, are used in the outer tank of washing machines. New grades of high-flow PPs are allowing manufacturers to mold high-performance housewares. Polypropylene films are used in a variety of packaging

applications. Both oriented and non-oriented films are used. Film tapes are used for carpet backing and sacks. Foamed sheet is used in a variety of applications including thermoformed packaging. Fibers are another important application for polypropylene, particularly in carpeting because of its low cost and wear resistance. Fibers prepared from polypropylene are used in both woven and non-woven fabrics [21].

2 NUCLEATION

Primary nucleation is the precursor of crystal growth and of overall crystallization processes. Crystallization in polypropylene starts at seeds which pre-exist or are formed in molten PP. Seeds give rise to crystal lamellae which grow then radially to form discs or spheres, forming crystalline aggregates called spherulites. At later stages, growing spherulites impinge and form a spherulitic structure. The classical concept of crystal nucleation is based on the assumption that fluctuations in the supercooled phase can overcome the energy barrier at the surface of the crystal [13].

The crystallization of iPP from melt could be enhanced in the temperature region where heterogeneous nucleation is observed by adding some extra heterogeneous nuclei. The interest in such procedure was stimulated by industrial efforts to decrease the size of spherulites for improvement of transparency and mechanical properties. By adding finely subdivided foreign material, it was shown that solids, liquids, and even gas bubbles, are able to nucleate PP spherulites [9]. The addition of nucleating agents provides a large number of sites for the initiation of crystallization, so that spherulites formed are smaller and more numerous than in unnucleated polypropylene. Nucleation increases the crystallization temperature and the rate of crystallization [10].

Nucleated materials have usually higher tensile strength, stiffness, flexural module and heat deflection temperatures than unnucleated materials, but impact strength is lower [6]. The high levels of crystallinity can result in reduced tolerance to radiation sterilization as compared to unnucleated polypropylene, and the effectiveness of hindered amine light stabilizers and other stabilizing additives can be reduced. Clarity is enhanced due to the increased cooling rate and the decreased spherulite size, which reduces the scattering of light as it passes through the material. Smaller spherulites can reduce warpage in some applications and can provide a harder, more stainresistant surface [10].

Nucleating agents used in polypropylene include carboxylic acid salts, benzyl sorbitols, and salts of organic phosphates. All these nucleating agents cause the crystallization into monoclinic α-phase. Carboxylic acid salts provide limited clarity enhancement but do enhance the mechanical properties by an increase in the crystallization

rate. Dibenzylidene sorbitols reduce crystal size dramatically, resulting in greatly improved clarity. Benzyl sorbitols can result in odor generation during processing which produces odor in the finished part. Pigments, such as phthaloxyanine blue and green and phthalyl blue, and mineral fillers such as talc can also act as nucleating agents, although talc is not taken as effective [8].

Sorbitol-based nucleators provide significant improvement over conventional nucleating agents in both nucleating efficiency and clarity. The most common examples of this type are 1,2,3,4-bis-dibenzylidene sorbitol (DBS) and 1,2,3,4-bis-(*p*-methoxybenzylidene) sorbitol (DOS). The major drawback of DBS is its fast evaporation rate during processing. Modified structures of DBS such as 1,2,3,4-bis-(*p*-methylbenzylidene) sorbitol (MDBS) and 1,2,3,4-bis-(3,4-dimethylbenzylidene) sorbitol have been developed to solve this problem and improve the nucleating efficiency. The sorbitol derivative 1,2,3,4-bis-(3,4-dimethylbenzylidene) sorbitol (DMDBS), commercially known as Millad 3988, is the most successful clarifying agent (Fig. 2.1.) [29].

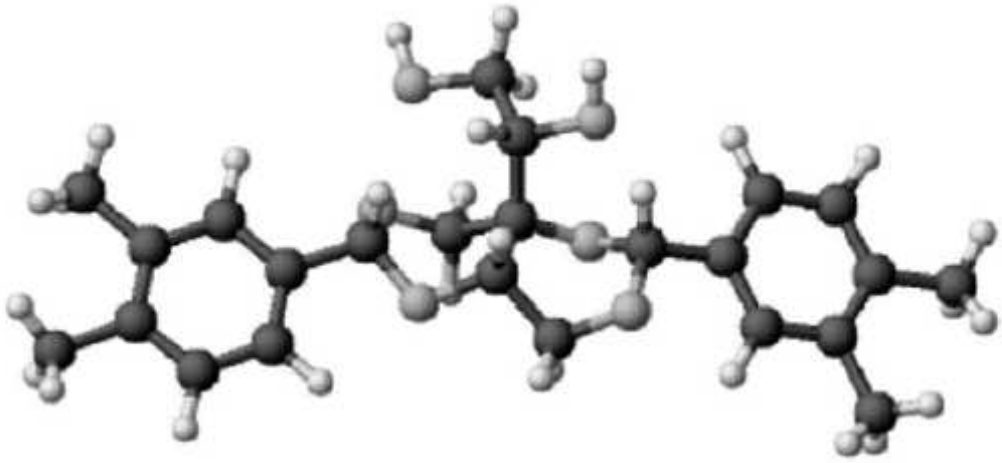

Fig. 2.1: Three-dimensional optimalization of DMDBS chemical structure [29]

Unlike the dispersion-type nucleators, it dissolves in the molten PP and disperses uniformly in the matrix. When the PP cools, the nucleator first crystallizes in the form of a three-dimensional fibrillar network of nanometric dimensions. The nanoscale fibril network serves as nucleating sites for PP, due to its large surface area, leading to enhanced nucleation of small polymer crystals [29].

3 PHOTODEGRADATION

Polyolefins are often used for outdoor applications. By virtue of the weather conditions, the material age and change its properties (embrittlement, cracking of the surface, color changes, decrease of the mechanical features etc.) Weathering of polymers may be caused by various factors as for example mechanical stress, oxidation, heat- or biodegradation. One of the most severe factors contributing to degradation is ultraviolet radiation.

The process of the degradation caused by solar radiation, usually ultraviolet radiation (UV) is called UV-degradation or photodegradation. Considering the mechanism and the conditions of the reactions the oxygen takes place indeed, when gear the reactions. That means that in normal conditions when the polymers are used the provisions for the degradation caused by the UV-light and the oxygen together have to be made. This type of degradation is called photooxidative degradation (photooxidation). A lot of polymeric materials are, more or less, sensible to the act of UV radiation. For iPP the UV-degradation is the most considerable type of the degradation.

3.1 Photophysics

Visible light, infrared, ultraviolet, and γ-rays are each a distinct form of electromagnetic radiation (Fig. 2.1). Each propagates in space as waves of electronic and magnetic fields. Electromagnetic waves carry a discrete amount of energy depending on their frequency, as stated by Planck's Law [22]:

$$E = h\nu \qquad (1)$$

where E = energy of radiation [J]

ν = frequency of radiation [1/s]

h = Planck's constant [J.s]

The frequency of radiation depends on the conditions in which this radiation was formed. With a temperature increase, the light spectrum is shifted to the left, meaning that more UV and visible light is emitted [22].

It is evident that radiation with higher frequency, ergo with lower wavelength, carries a greater amount of energy. At the earth's surface lies the most energetic solar radiation in region of ultraviolet wavelength in electromagnetic spectrum.

Ultraviolet wavelengths from sunlight are an important component in outdoor degradation. The energy from sunlight is mainly visible and infrared light; ultraviolet makes up less than 5 % of sunlight. However, the photodegradation of exterior plastic materials is caused mainly by UV-light (Fig. 3.1.1).

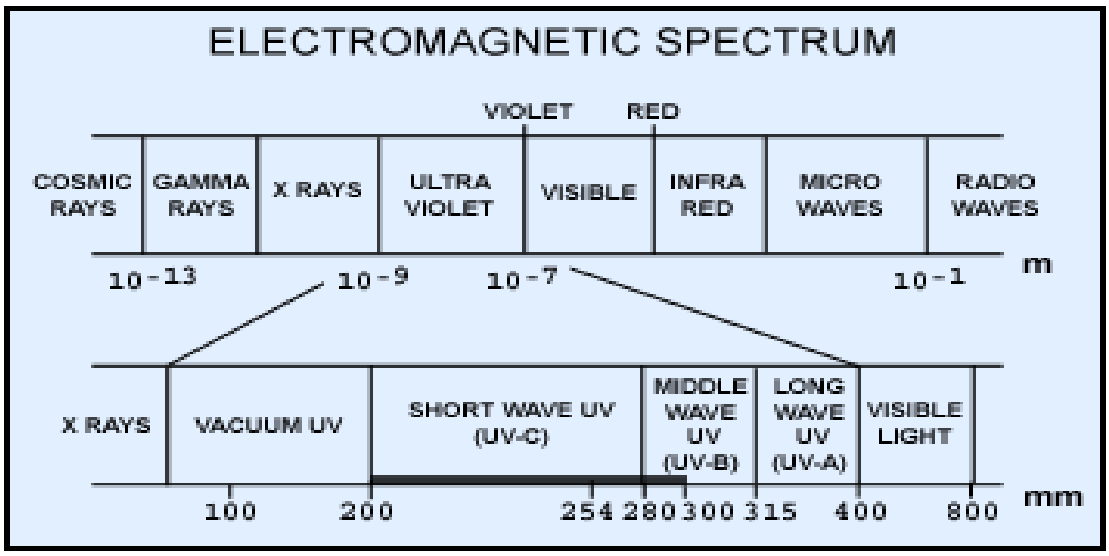

Fig. 3.1.1: Electromagnetic spectrum

Under normal conditions, most organic molecules are in the ground state (S_0). The lowest energy state for these molecules is a singlet state in which electrons with opposing spins are paired in the molecular orbitals. The frequently-used Jablonski diagram shows the possible outcomes when molecules absorb energy (Fig. 3.1.2) [22].

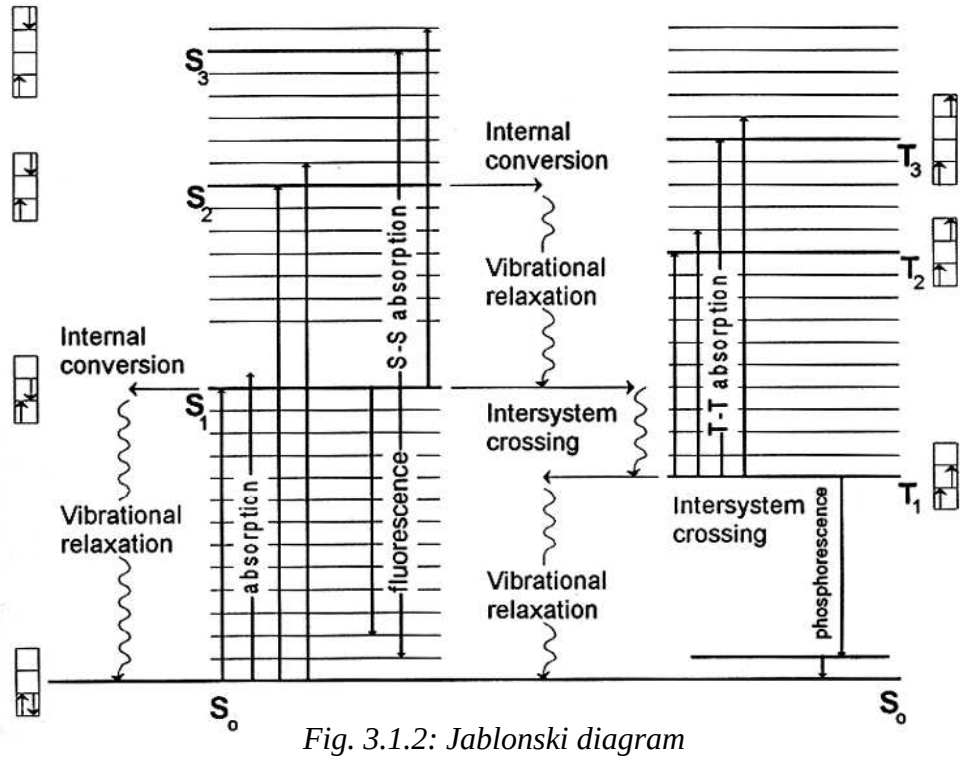

Fig. 3.1.2: Jablonski diagram

At first electrons in molecule of polymer absorb the radiation energy. Depending on the energy absorbed by the molecule, the electrons are promoted from ground state to higher energy state levels. The absorbed energy is then dissipated either in radiative processes as fluorescence and phosphorescence or in non-radiative processes. In them is absorbed energy converted. This process, in dependence on the balance of energy available in a particular molecule and in the chemical structure of the excited molecule, can lead to cleavage into free radicals, abstraction of hydrogen atom, photosensitization, decomposition with formation of two or more molecules, photodimerization or crosslinking, intramolecular rearrangement or photoizomerization. Which reaction type predominates partly depends on the environment. These primary photochemical reactions are mostly followed by secondary reactions; prevailingly with oxygen or ozone and photooxidation is realized [22].

3.2 Photochemistry

Most commercial organic polymers undergo chemical reaction upon irradiation with ultraviolet light, because they posses chromophoric groups (as regular constituents or as

impurities) capable of absorbing UV light. Carbonyl groups play a prominent role among these chromophoric groups [23]. Therefore, the photochemistry of ketone polymers was selected to demonstrate how light-induced chemical reactions proceed. As can be seen from Fig. 3.2.1, light absorbed by carbonyl groups can include bond scission by either Norrish type I or type II processes.

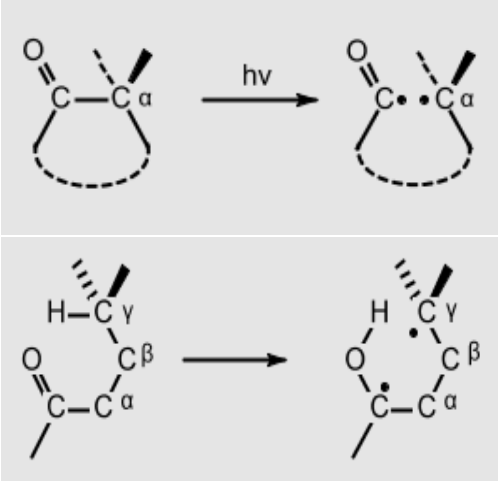

Fig. 3.2.1: Norrish I and II reactions [24]

The fraction of absorbed photons, utilized for chemical transformation, depends significantly on polymer mobility. The importance of molecular mobility derives from the fact that in type II processes the close approach of excited carbonyl groups to H atom at γ-carbons is a prerequisite for reaction. Moreover, cage recombinations of radical pair (produced e.g. in type I processes) become less probable, as the mobility increases [23].

The most common photoreaction for all materials is photooxidation. Usually, free radicals are generated as transient species in photolytic processes. Since oxygen reacts readily with most free radicals, peroxyl radicals will be formed. Photolysis, therefore, can give rise to autoxidative free radical chain reaction. The primary reaction steps are following (Fig. 3.2.2):

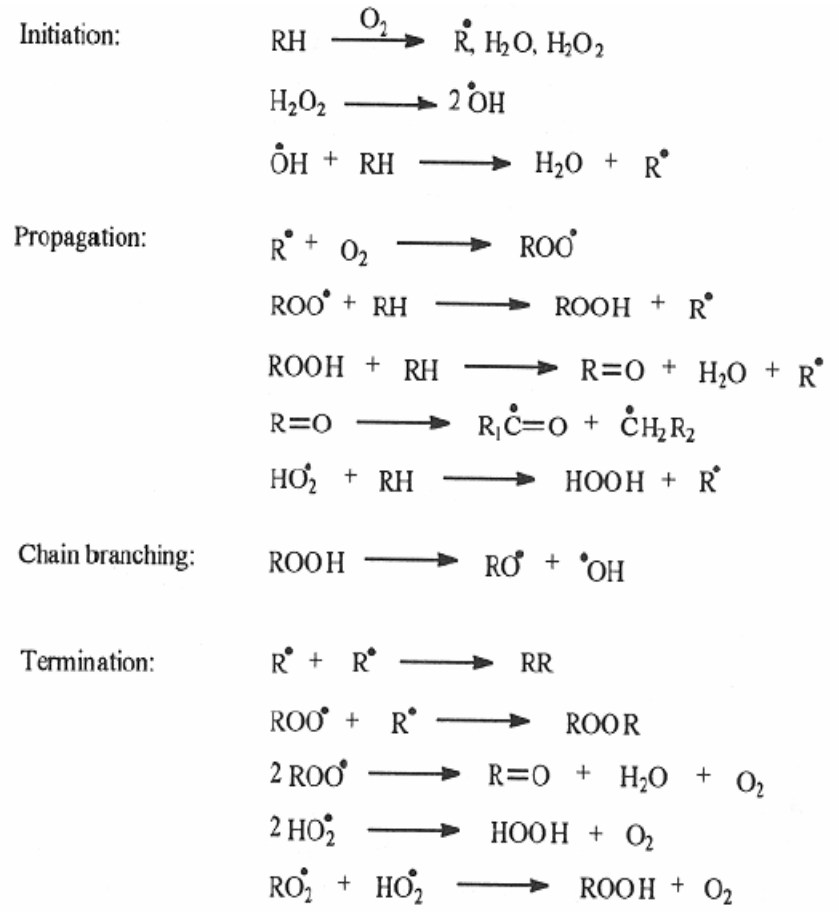

Fig. 3.2.2: Photooxidation of polyolefins [24]

Hydroperoxide groups are formed in the propagation reaction. At wavelengths below 300 nm hydroperoxides are photolytically decomposed (Fig 3.2.3).

ROOH + hν → RO· + ·OH

Fig. 3.2.3: Formation of hydroperoxide groups

This reaction is considered to be very important in the photoinitiated oxidation of many commercial polymers because of presence of peroxide groups as chemically bound impurities, originating from processing at elevated temperature in the presence of oxygen [23].

3.3 Photodegradation of Polypropylene

The degradation mechanism of polypropylene is very similar to other polyolefins. The primary events following irradiation of polypropylene with UV light in vacuum are bond scission and crosslinking (Fig. 3.3.1) [22, 25].

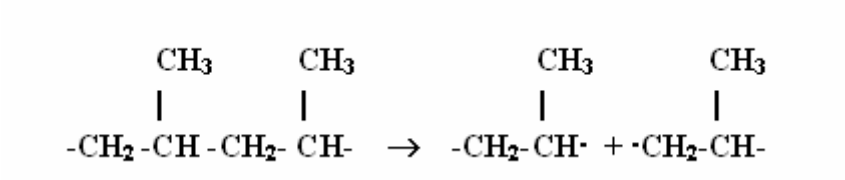

Fig. 3.3.1: Chain scission of PP

Another probable reaction is the dissociation of carbon-hydrogen bonds at the tertiary carbon (Fig 3.3.2).

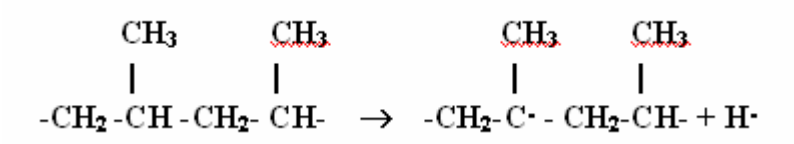

Fig. 3.3.2: Dissociation of carbon-hydrogen bonds

This may lead to chain scission by a disproportionation reaction (Fig 3.3.3) [25].

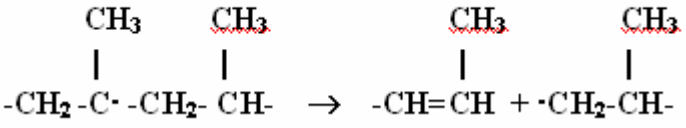

Fig. 3.3.3: Chain scission of PP by a disproportionation reaction

When two polypropylene radicals react crosslink is formed (Fig. 3.3.4).

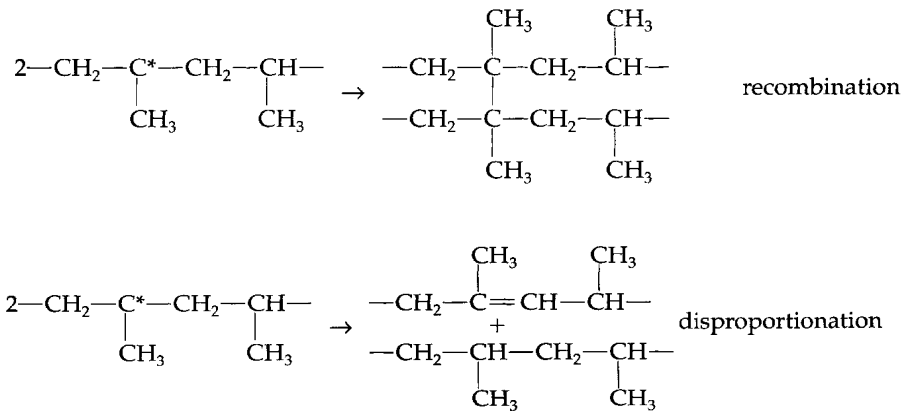

Fig. 3.3.4: Crosslinking of polypropylene radicals [26]

Degradation reactions during outdoor exposure are others then during irradiation in vacuum. Saturated hydrocarbon polymers (e.g. 'pure' PP) are intrinsically transparent to the incident sun spectrum and should not be affected by the solar radiation. Commercial PP, however, absorbs weakly at wavelengths above 285 nm and its sensitivity to sunlight is a consequence of light absorbing impurities, particularly oxygen-containing species and other species present arising from production processes, i.e. polymer manufacture, melt processing and fabrication. These impurities sensitize and accelerate PP photooxidative degradation under service conditions involving exposure to light (outdoors and indoors) resulting in changes of properties [27].

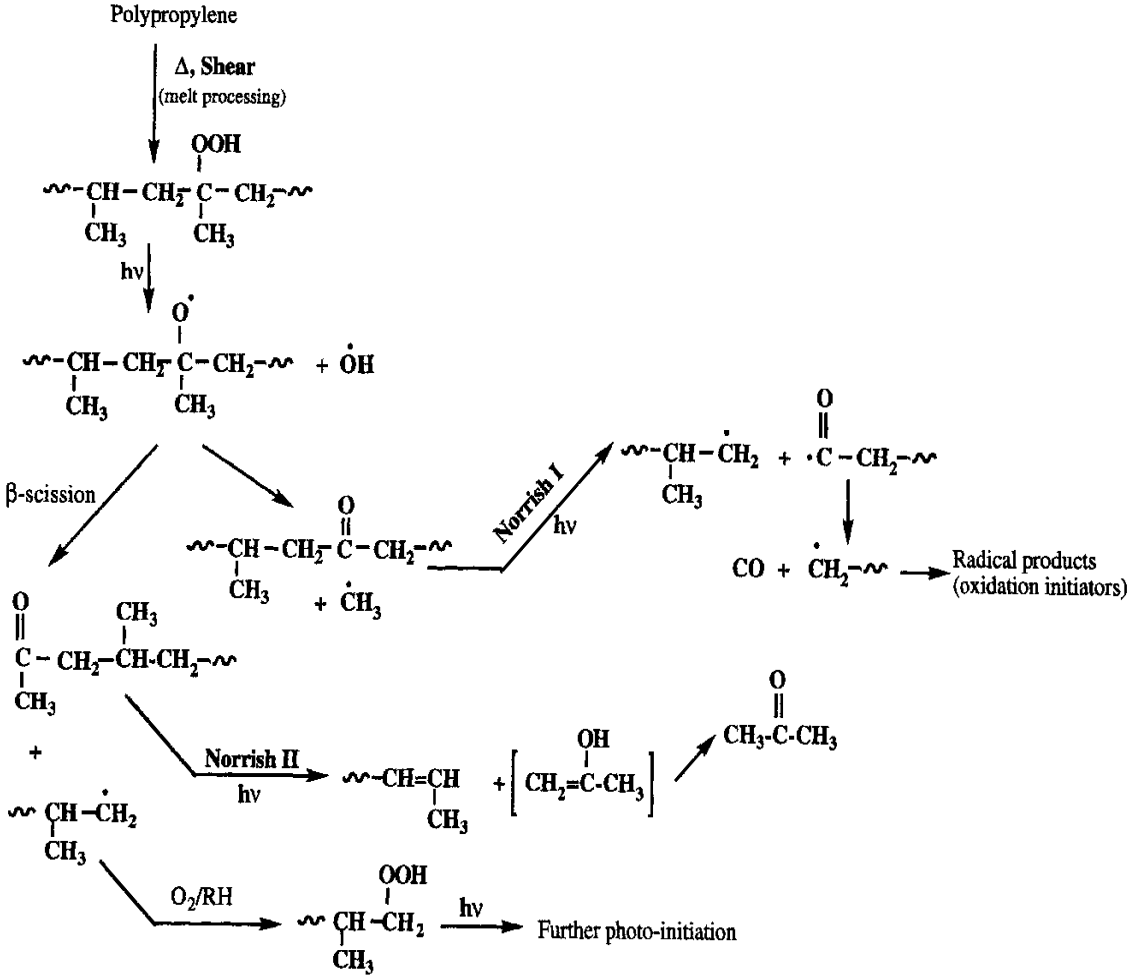

Fig. 3.3.5: Polymer hydroperoxidation during processing and further photoinitiation by the hydroperoxides and the derived carbonyl compounds [31]

Hydroperoxides formed during melt processing are the most important impurities (photoinitiators). They play a major initiating role during the early stages of PP photooxidation, while the derived carbonyl-containing products exert deleterious effects during later stages of photooxidation (e.g. by Norrish types I and II reactions), see Fig. 3.3.5. Hydroperoxides and their decomposition products are responsible for the changes in molecular structure and overall molar mass of PP which are manifested in practice by the loss of mechanical properties and by changes in the physical properties of the polymer surface [27].

A higher temperature of oxidation speeds both the formation rate and the decomposition rate of hydroperoxides. When carbonyl concentration is high, the rate of formation of hydroperoxides is dependent on the initial thermooxidative processes. As a result of photodegradation, more ester groups are formed and an aldehyde group is also generated. Carbonyl groups and hydroxyl groups are preferentially formed on the exposed surface, and their concentrations increase almost linearly with time of exposure.

3.4 Effect of Morphology on Photodegradation

The process of degradation of PP depends on the physical structure, as well as for other semicrystalline polymers. Degree of crystallinity strongly influences the degradation kinetics. The higher is the crystallinity, the lower is the oxygen permeability and thus the lower is the rate of oxidation.

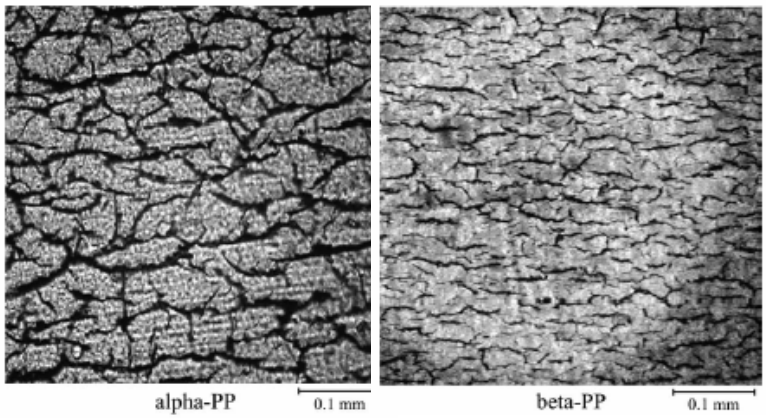

Fig. 3.4: Surface cracks on α-PP and β-PP specimens after 240 h UV exposure [28]

The effect of PP polymorphism on the degradation of polypropylene (especially induced by UV-irradiation) is also observed. It is found, that the β-nucleation specifically affect the processes of UV degradation of isotactic polypropylene [28]. The molecular degradability of β-nucleated polypropylene is lower as compared to common α-polypropylene. Figure 2.17 shows the micrographs of surfaces of degraded α-iPP and β-iPP. Deep and relatively distant macroscopic cracks on the surface of α-iPP specimen are seen while the surface of β-iPP is damaged by a dense network of fine cracks, only microscopically observable [28].

4 EXPERIMENTAL METHODS

4.1 Accelerated Weathering Test

Most data on the ageing of plastics are acquired through accelerated tests and actual outdoor exposure. The latter is a time-consuming method; accelerated tests are often used to expedite screening the sample with various combinations of additive levels and ratios. A variety of light sources are used to simulate the natural sunlight. The artificial light sources include carbon arc lamps, xenon arc lamps, fluorescent sun lamps, and mercury lamps. These light sources, except the fluorescent, are capable of generating a much higher light intensity than natural sunlight [30].

Fig. 4.1: Accelerated weathering device [31]

A laboratory environment is chosen as a suitable place to conduct experiments for a variety of reasons [22]:

- conditions are well controlled;
- more precise detection instruments are available;
- the environment is clean so contamination can be eliminated or accurately controlled;
- small samples can be used, waste can be minimized, cost per experiment can be minimized, experienced labor is available, less labor is needed than in field testing simultaneous experiments can be carried out giving faster results.

A scientist working on material degradation (weathering) uses laboratory because [22]:

- accelerated test gives results sooner than would be obtained by outdoor weathering;
- outdoor conditions are too variable and cannot be controlled;
- samples exposed outdoors become contaminated and they are unsuitable for some instrumental analysis.

4.2 Differential Scanning Calorimetry

Differential scanning calorimetry (DSC) measure the rate and degree of heat change as a function of time or temperature. In addition to these direct energy measurements, the precise temperature of the sample material at any point during the experiment is also monitored. Since DSC can measure both temperatures and heats of transitions or reactions, it has replaced differential thermal analysis (DTA) as the primary thermal analysis technique, except in certain high-temperature applications [32].

The basic principle underlying this technique is that, when the sample undergoes a physical transformation such as phase transitions, more (or less) heat will need to flow to it than the reference to maintain both at the same temperature. Whether more or less heat must flow to the sample depends on whether the process is exothermic or endothermic. For example, as a solid sample melts to a liquid it will require more heat flowing to the sample to increase its temperature at the same rate as the reference. This is due to the absorption of heat by the sample as it undergoes the endothermic phase transition from solid to liquid. Likewise, as the sample undergoes exothermic processes (such as crystallization) less heat is required to raise the sample temperature [32−34].

In a cell designed for quantitative DSC measurements, two separate sealed pans, one containing the material of interest and the other containing an appropriate reference, are heated (or cooled) uniformly (Fig. 4.2.1) [32]. The DSC cell uses a constantan disk as the primary means of transferring heat to the sample and reference holders and also as one element of the temperature-sensing thermoelectric junction. Samples in powder, sheet, film, fiber, crystal, or liquid form are placed in disposable aluminum sample pans of high thermal conductivity and weighed on a microbalance. The sample is placed in one

sample holder and an empty sample holder serves as reference. Sample sizes range from 0.1 to 100.0 mg [32].

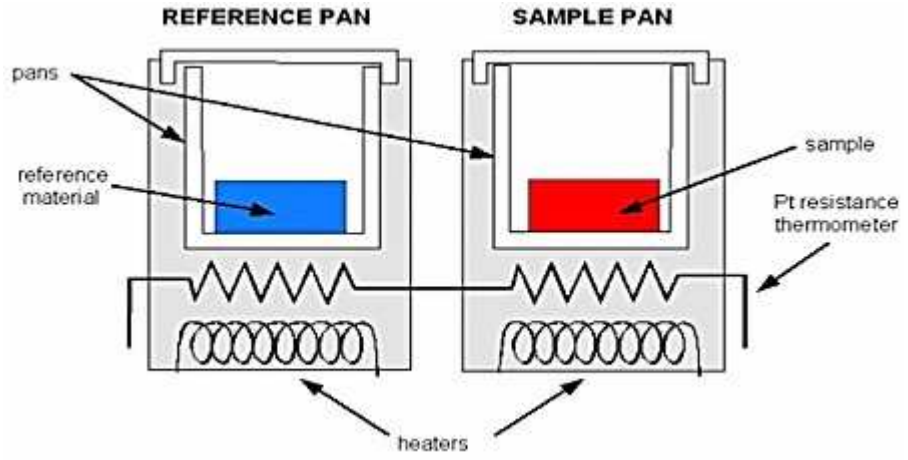

Fig. 4.2.1: Schematic diagram of differential scanning calorimetry [35]

The result of a DSC experiment is a heating or cooling curve (Fig. 4.2.2). This curve can be used to calculate enthalpies of transitions. This is done by integrating the peak corresponding to a given transition.

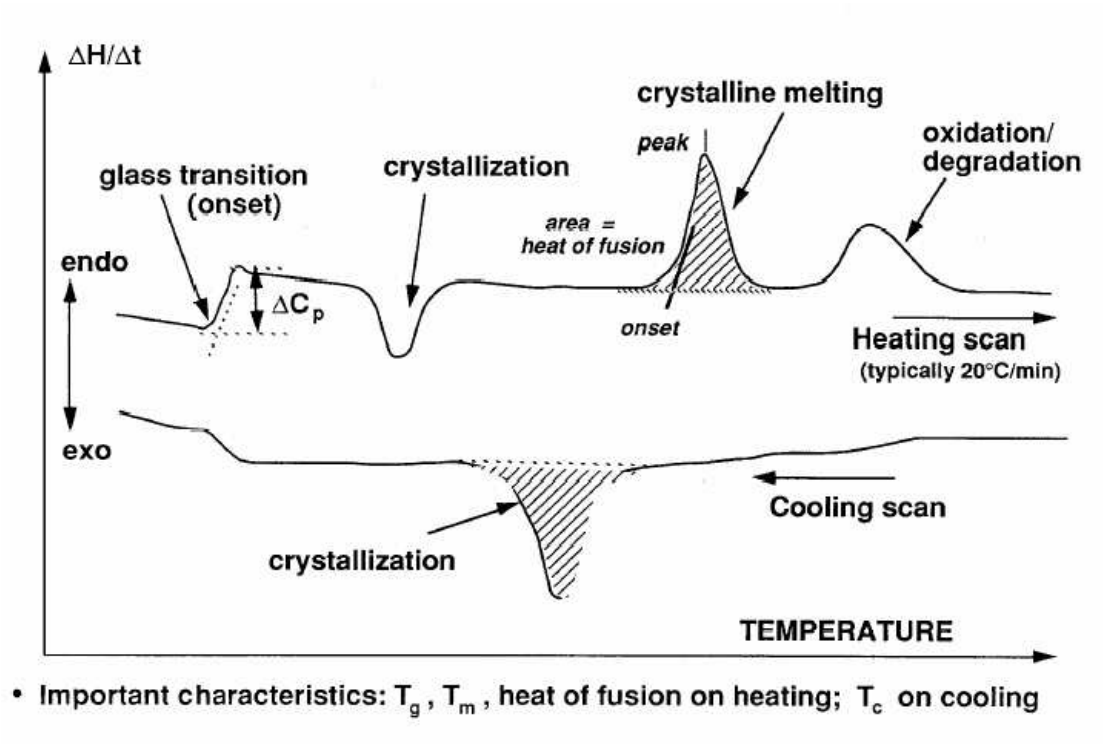

Fig. 4.2.2: Typical polymer DSC thermogram [36]

4.3 X-ray Diffraction

X-ray Diffraction (XRD) is a powerful technique used to uniquely identify the crystalline phases present in materials and to measure the structural properties (strain state, grain size, epitaxy, phase composition and defect structure) of these phases. XRD is also used to determine the thickness of thin films and multilayers, and atomic arrangements in amorphous materials (including polymers) and at interfaces [37]. Other information which can be obtained by X-ray diffraction includes crystal size and perfection, the long period in lamellar polymers (= lamellar thickness + interlamellar region), crystallinity, the degree of preferred orientation in polycrystalline samples, and, in some recent studies, the conformation of chains in amorphous polymers has been determined as well [38].

The principle is diffraction (viewed in Fig. 4.3) of the X-ray radiation beams on the regular structure consequently on the crystal lattice. The crystal diffracts an X-ray beam passing through it to produce beams at specific angles depending on the X-ray wavelength (about 10 nm), the crystal orientation and the structure of the crystal [39].

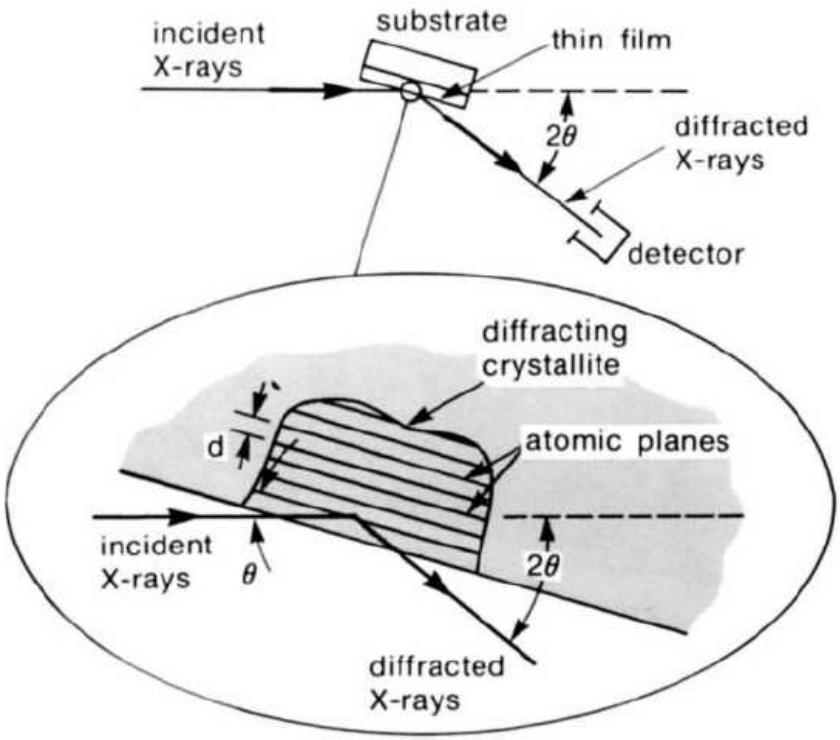

Fig. 4.3: Basic features of a typical XRD experiment [37].

X-rays are scattered when interacting with the electrons in the atoms. If the atoms are organized in planes (the matter is crystalline) and the distances between the atoms are of the same magnitude as the wavelength of the X-rays, constructive and destructive interference occurs and a diffraction pattern forms. A diffraction pattern records the X-ray intensity as a function of 2θ angle (θ angle is the angle of diffraction and for practical reasons this angle as measured by diffractometer twice – 2θ angle). The distance between similar atomic planes in the interatomic spacing is called the *d*-spacing and measured in nm. The wavelength of the incident X-radiation is symbolized by the Greek letter lambda λ and *n* is an integer [40]. These factors are combined in Braggs law:

$$n\lambda = 2d\sin(\theta) \tag{2}$$

XRD is an excellent, noncontact and nondestructive method for identifying phases and characterizing the structural properties of thin films and multilayers which makes it ideal for in situ studies. It is inexpensive and easy to implement [37].

4.4 Infrared Spectroscopy

The physical principles underlying infrared spectroscopy have been appreciated for more than a century. As one of the few techniques that can provide information about the chemical bonding in a material, it is particularly useful for the nondestructive analysis of solids and thin films, for which there are few alternative methods. Liquids and gases are also commonly studied, more often in conjunction with other techniques [37].

Infrared (IR) radiation is electromagnetic radiation in the wavelength range 0.78–1 000 mm which corresponds to the wave number range 12 800–10 cm^{-1} The IR portion is usually divided into near- (13 000–4 000 cm^{-1}), mid- (4 000–200 cm^{-1}) and far-IR region (200–10cm^{-1}), whereas most widely used is mid-IR region [41].

A beam of IR light is passed through a sample, and the amount of energy absorbed at each wavelength is recorded [42]. In an output IR spectrum energy is plotted as a function of a wavelength.

IR radiation can only been absorbed by bonds within a molecule, if the radiation has exactly the right energy to induce a vibration of the bond. This is the reason why only specific wavelengths are absorbed [43]. Radiation is absorbed resulting in a series of peaks in the spectrum, which can then be used to identify the sample. Peaks in the spectrum can be also used for quantitative analysis of some organic compounds. A wavelength of light which has been absorbed is characteristic of the chemical bond. Therefore, the chemical bonds in a molecule can be determined by interpreting an IR absorption spectrum [44].

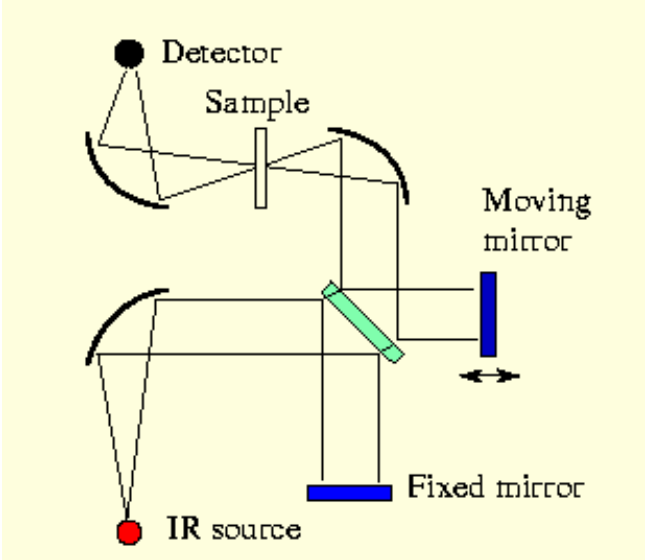

Fig. 4.4: Schematic sketch of the essential features of a Fourier transform infrared spectrometer [45]

Fourier-Transform Infrared (FT-IR) Spectrometer (Fig. 4.4). The FT-IR spectrometer provides speed and sensitivity. A Michelson interferometer, a basic component, consists of two mirrors and a beam splitter. The beam splitter transmits half of all incident radiation from a source to a moving mirror and reflects half to a stationary mirror. Each component reflected by the two mirrors returns to the beam splitter, in which the amplitudes of the waves are combined either destructively or constructively to form an interferogram as seen

by the detector. By means of algorithms the interferogram is Fourier-transformed into the frequency spectrum. This technique has several distinct advantages:

1. The FT-IR spectrometer scans the infrared spectrum in fractions of a second at moderate resolution, a resolution that is constant throughout its optical range. It is especially useful in situations that require fast, repetitive scanning (for example, in gas or high-performance liquid chromatography).

2. The spectrometer measures all wavelengths simultaneously. Scans are added. The signal is N times stronger and the noise is N1/2 as great, so the signal-to-noise advantage is N1/2.

3. An interferometer has no slits or grating; its energy throughput is high, and this means more energy at the detector where it is most needed [32].

4.5 Optical Stereomicroscopy

Stereomicroscopy is used for three dimensional imaging where the perception of depth and contrast is critical to the interpretation of specimen structure. The wide field of view and variable magnification of stereomicroscopes lend them for application in both industrial assembly and in biological research for the manipulation of delicate and sensitive living organisms [46].

The human eyes and brain function together to produce what is referred to as stereoscopic vision, which provides spatial, three-dimensional images of the objects. This is because of the brain's interpretation of the two slightly different images received from each of the retinas. The average human eyes are separated by a distance of approximately 64−65 mm, and each eye perceives an object from a somewhat different viewpoint that differs by a few degrees from the other. When transmitted to the brain, the images are fused together, but still retain a high degree of depth perception, which is truly remarkable. The stereomicroscope takes advantage of this ability to perceive depth by transmitting twin images that are inclined by a small angle (usually between 10 and 12 degrees) to yield a true stereoscopic effect [47].

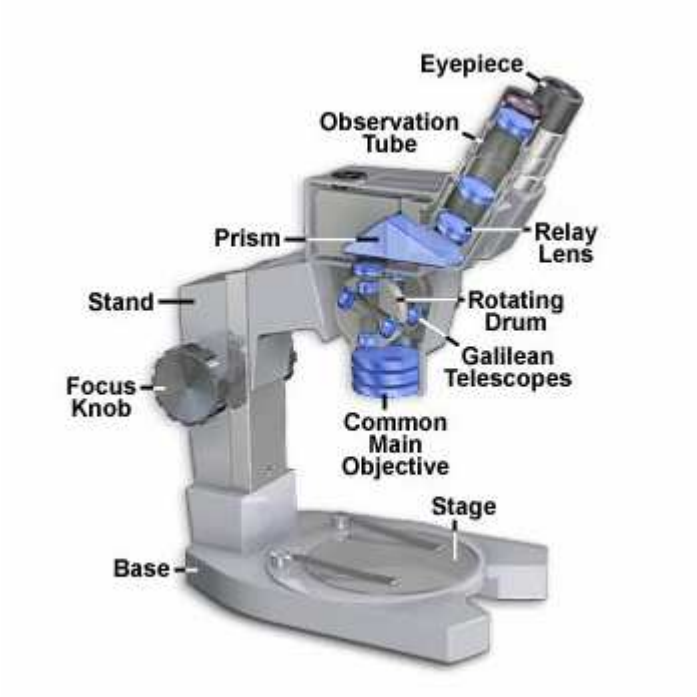

Fig. 4.5: Optical stereomicroscope configuration [47]

Stereomicroscopes are used to examine specimens under both reflected (episcopic) and transmitted (diascopic) light. Often transmitted and reflected light sources are combined to take advantage of particular specimen features to best reveal its characteristics.

There are three main techniques for the stereoscopic illumination of specimens:

Oblique Illumination – useful for specimens that are nearly transparent or colorless, where regular brightfield illumination is insufficient. Greater contrast and visual clarity can be achieved with illumination directed from a single source which strikes the specimen at an oblique angle.

Darkfield Illumination – requires a specialized stand containing a reflection mirror and light shielding plate, these act to direct an inverted hollow cone of light, at oblique angles towards the specimen. The principles behind darkfield illumination are similar in stereomicroscopy as regular compound microscopes.

Fluorescence (GFP) Illumination – With applications in both biological and industrial work, stereomicroscopes are used widely in GFP observation and are known as GFP illuminators [46].

II. EXPERIMENTAL PART

5 MATERIALS

The basic material used throughout this study was isotactic PP Mosten GB 005 manufactured by Chemopetrol Litvínov a. s., the Czech Republic. Polypropylene Mosten GB 005 is a general purpose homopolymer, intended for injection moulding and for production of thermoforming films. It can be also used for production of various compounds. This polymer is intended for preparing uniaxially oriented tapes and fibres. Some characteristics of this material featured by producer are shown in Table 5.1. The material is stabilised by a standard package based on phenol-phosphite stabilizers.

Table 5.1: Characteristic of PP MOSTEN GP 005

Property	Unit	Typical value	Test method
MELT FLOW RATE (230/ 2,16)	g/10 min	5	ISO 1133
YIELD STRESS	MPa	35	ISO 527
ELOGATION AT BREAK	%	>100	ISO 527
FLEXURAL MODULUS	MPa	1600	ISO 178
CHARPY NOTCHED IMPACT STRENGHT 23°C	kJ/m ^{2}	4	ISO 179
CHARPY NOTCHED IMPACT STRENGHT -20°C	kJ/m ^{2}	-	ISO 179
VICAT SOFTENING TEMPERATURE	°C	157	ISO 306
HDT (1,8 MPa)	℃	57	ISO 75
M_n	g/mol	65 600	-
M_w	g/mol	360 000	-
M_z	g/mol	1 050 000	-
M_w/M_n	-	5.6	-
ISOTACTICITY INDEX	%	98	ISO 9113

In order to increase the transparency in the samples, specific α-nucleating agent Millad 3988 produced by Milliken Chemical was used. It is 1,3:2,4-di(3,4-dimethylbenzylidene) sorbitol, with the chemical formula shown in Fig. 5.1.

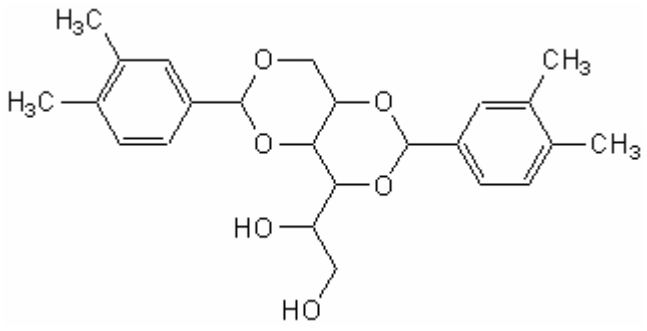

Fig. 5.1: Chemical structure of Millad 3988

6 BLENDS PREPARATION

For the purpose of the study three blends of PP were used and, for comparison, also the neat PP was studied. The concentrations of α-nucleating agent Millad 3988 in the blends were 0.2, 0.5 and 0.8 wt.%. For better dispergation of the nucleating agent 0.3 wt.% of paraffin oil were used. The composition of the blends is given in Table 6.1.

Table 6.1: Composition of blends

Blend No.	Nucleator		Polypropylene		Parafin Oil			Suma
	wt. %	(g)	wt. %	(g)	wt. %	(g)	(ml)	(g)
1	0	0	100	2250.00	0	0	0	2250
2	0.2	4.50	99.5	2238.75	0.3	6.75	7.759	2250
3	0.5	11.25	99.2	2232.00	0.3	6.75	7.759	2250
4	0.8	18.00	98.9	2225.25	0.3	6.75	7.759	2250

Paraffin oil and subsequently nucleating agent were manually immixed into iPP pellets. Blends were then processed using twin-screw extruder Brabender DSK 42/6D and finally pelletized.

Processing prameters of extruder: feed section…….180 °C
transition section.....200 °C
metering section…..210 °C
screw speed…….60 min^{-1}

7 SAMPLES PREPARATION

Samples for X-ray scattering, DSC and polarized light microscopy were prepared from produced pellets.

Samples for Xenotest, X-ray scattering, DSC, FTIR and optical microscopy were prepared from the blends plates, which were compression-moulded using a manual press and mould with inside dimensions 125x60x0.2 mm at the following conditions:

• Temperature = 210 °C;
• Preheating time = 2 min;
• Pressing time = 5 min;
• Cooling time in a hydraulic press at temperature 20 °C = 5 min.

Samples with dimensions 30x10 mm were cut from the prepared plates. These samples were placed into steel frames which were compatible with Xenotest, X-ray difractometer and Infrared spectrometer (Fig. 7.1).

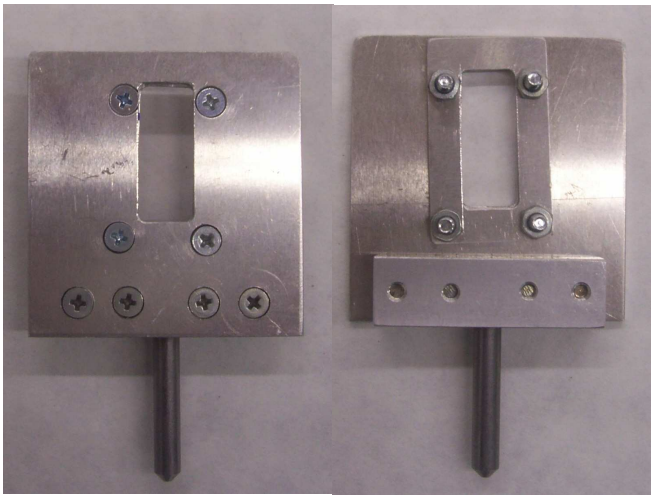

Fig. 7.1: Clamp holder for irradiated samples

The samples for DSC measurements were taken from UV-irradiated specimens. The samples of weight of approx. 5 mg were put into the aluminium pan and covered with the aluminium cover. The pan and the cover were crimped with a special tool supplied by Perkin-Elmer.

8 METHODS AND DEVICES

8.1 Accelerated Weathering Test

The specimens were irradiated in Original Hanau XENOTEST® 150 at 50±5 °C (Fig. 8.1.1). The light source is the Xenon lamp Xe 1500, the light from which both in the visible region (400−700 nm) of the spectrum and in ultraviolet region (300−400 nm), approximates very closely to sunlight. A test time of 24 hours in the Xenotest is equal to the radiation of about 10 days in the open air over the average during the year.

Fig. 8.1: Original Hanau XENOTEST® 150

During the irradiation the samples were carried in aluminium frames and the exposure was applied for 0, 12, 24, 36, 48, 60, 72, 96, 120, 144, 192, 240, 288, 336, 384, 432, 480 and 528 hours.

8.2 Differential Scanning Calorimetry

For the purpose of the crystallization studies, a differential scanning calorimeter Perkin-Elmer Pyris 1, was employed (Fig. 8.2.1). Nitrogen as a purge gas was used and constantly passed 20 ml/s through the heat sink and over the cells. The temperature calibration was performed using indium as a standard.

Fig. 8.2: Differential scanning calorimeter Perkin-Elmer Pyris 1

To obtain measurements for crystallization, samples of about 5 mg weight were heated from 50 ºC to 220 ºC at a heating rate of 10 ºC/min, melted at 220 ºC for 5 min in order to eliminate any previous thermal history of the polymer. Subsequently, they were cooled at cooling rate 10 °C/min to 100 °C. Such non-isothermally crystallized samples were then heated to 190 °C at rate 10 °C/min with a view to observe subsequent melting of the crystallized samples.

8.3 X-ray Diffraction

Wide angle X-ray scattering (WAXS) experiments were performed with a HZG 3 diffractometer equipped with CuK_α in a transmission mode. Radial scans of intensity vs. diffraction angle 2θ were recorded in the range of 10 to 30 º by steps of 0.05 º and length of step scan 5 s (Fig. 8.3.1).

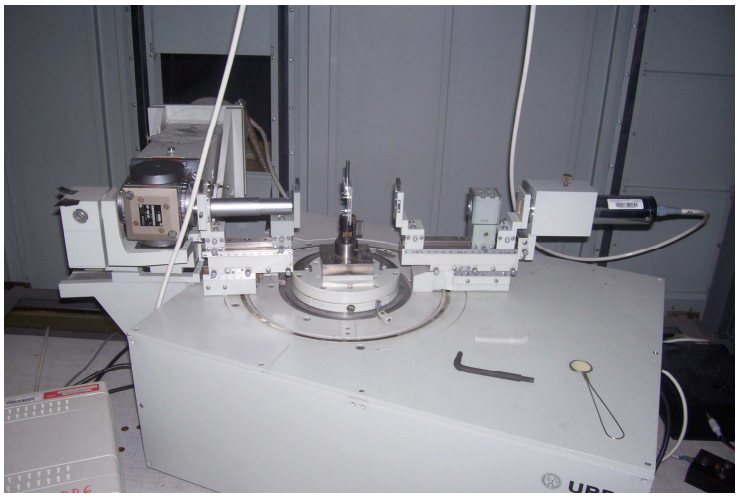

Fig. 8.3: HZG 3 diffractometer

8.4 Infrared Spectroscopy

The transmission FTIR spectroscopy analysis was applied on Nicolet, Impact 400 (Fig. 8.4.1), nominal resolution was 2 cm^{-1} and number of scans 64. FTIR was applied to determine chemical changes of the sample in the whole mid-infrared spectrum (4 000−500 cm^{-1}). This method was employed to analyze the amount of occurred carbonyl groups. In infrared spectra the carbonyl groups are expressed as a peak in the region of 1 700 to 1 800 cm^{-1}.

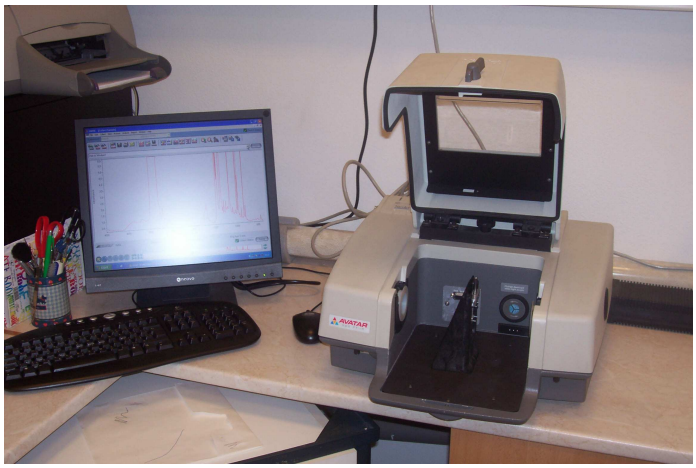

Fig. 8.4: Infrared spectrometer Nicolet Impact 400

8.5 Optical Stereomicroscopy

In order to study surface of the degraded samples, a Zeiss Stemi 2000-C microscope was used (Fig. 8.5.1). Micrographs of the observed surface were taken using a SONY F-717 digital camera.

Fig. 8.5: Stereomicroscope Zeiss Stemi 2000-C

III. RESULTS AND DISCUSSION

9 DIFFERENTIAL SCANNING CALORIMETRY

Differential scanning calorimetry was used to describe melting, re-crystallization and re-melting processes of irradiated samples. The values of melting temperatures, re-crystallization temperatures, re-melting temperatures and enthalpies of transitions are plotted in Appendice Nr. 1. Melting and crystallization temperatures are taken as a maximum of the peak.

9.1 Melting

Figs. 9.1.1 and 9.1.2 show melting thermograms of neat polypropylene and polypropylenes with different contents of nucleating agent. The melting thermograms do not significantly change in time interval from 0 to 240 hours. Peaks of neat polypropylene are rather flat (or splitted) and thus the exact value of melting temperature (T_{m1}) cannot be determined, only region of temperatures. The doubling can be explained by αα-recrystallization during heating. Application of the fast crystallization conditions leads to the creation of less regular and less stable structure. Subsequent slow heating can then cause the perfection of such structure [14].

Peaks of nucleated polypropylenes are sharp with perceptible maximum T_{m1}. Melting temperatures of nucleated polypropylenes vary only little with the concentration of nucleating agent. As for evolution of melting temperature within mentioned time interval (between 0 and 240 hrs) it does not change significantly. However, at prolonged exposure time (from 288 to 528 hours) melting temperatures of all samples continuously decreases. Moreover, the splitting of the peaks occurs. Finally, they are very flat with several maximums. The decrease of melting temperature is caused by erosion of the surfaces of the crystallites decreasing their thermodynamic stability [48].

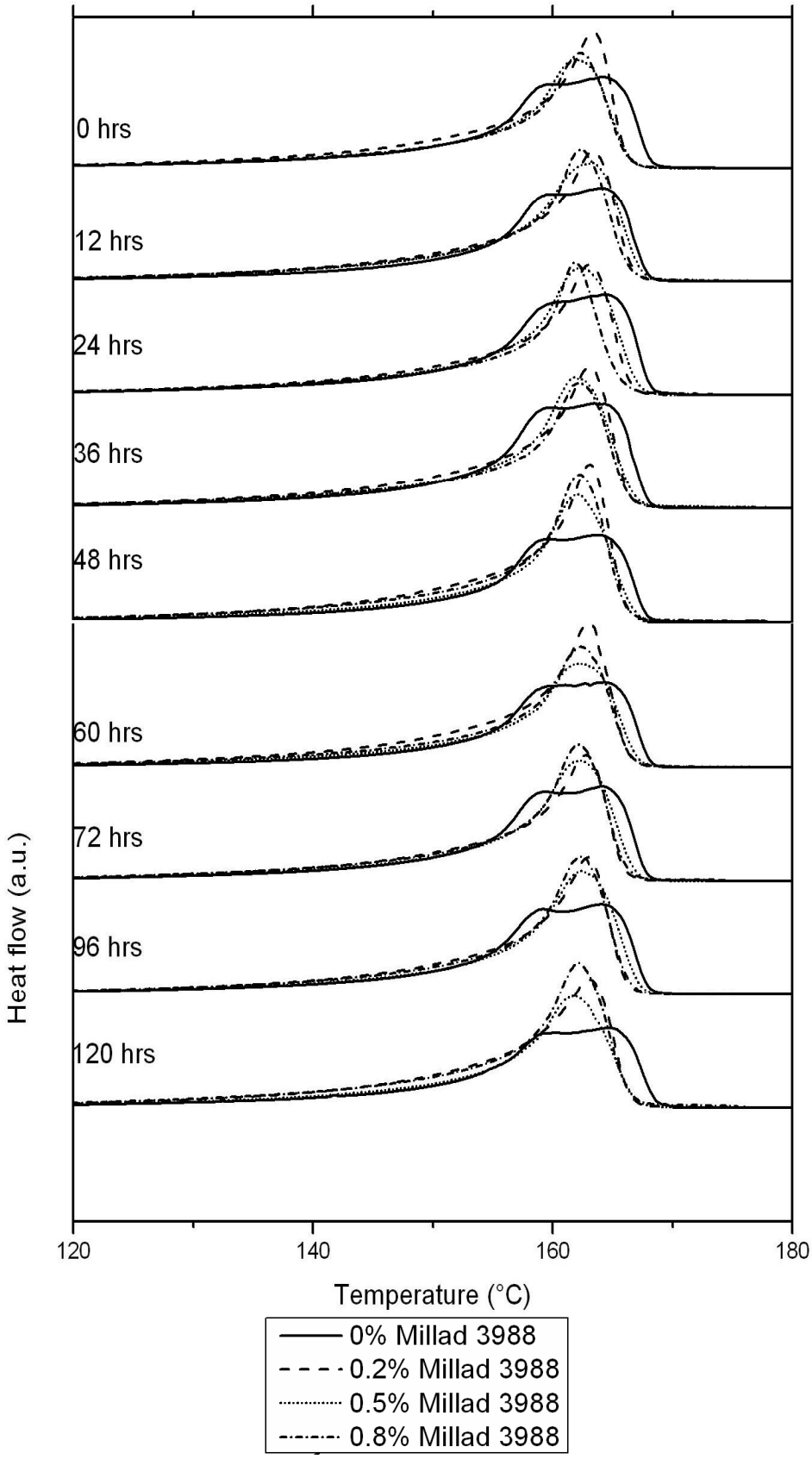

Fig. 9.1.1: Melting curves (0-120 hrs)

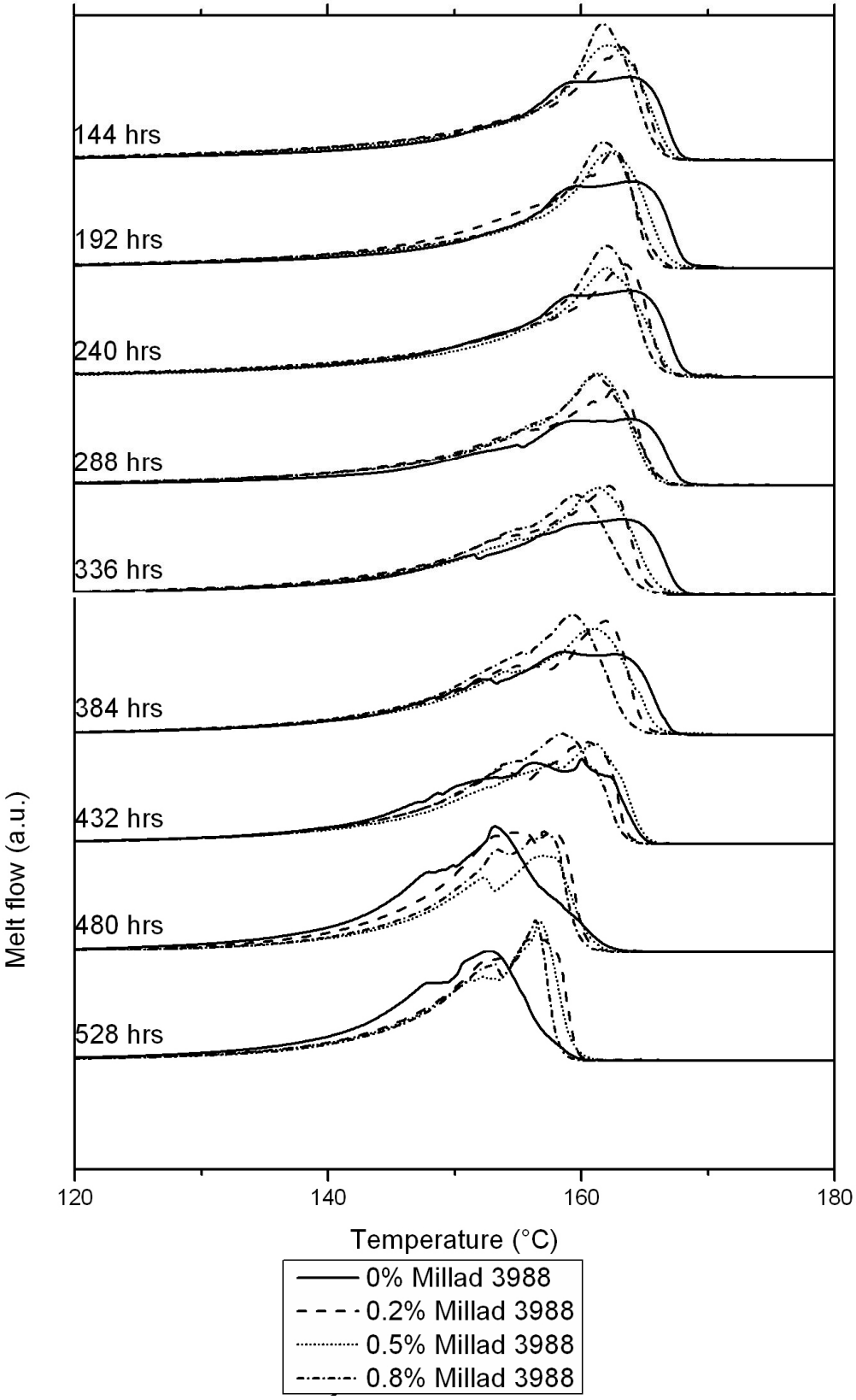

Fig. 9.1.2: Melting curves (144-528 hrs)

9.2 Re-crystallization

The melted polypropylene samples were then non-isothermally crystallized and the crystallization exotherms of each material are shown in Figs. 9.2.1 and 9.2.2. The evolution of the crystallization temperature (T_c) during UV-irradiation is displayed in Fig. 9.2.3. It can be seen that neat polypropylene crystallizes at significantly lower temperature (approx. 120 °C before irradiation) than nucleated polypropylenes (approx. 130 °C before irradiation). Indeed, the addition of heterogeneous nuclei into material accelerates the crystallization.

The evolution of T_c of all samples upon UV-exposure can be described as follows: At the beginning of UV-exposure (up to 100 hrs) the crystallization temperature little increases or decreases or remains stable. Than (up to 240 or 384 hrs depending on the concentration of nucelating agent) it gradually decreases and subsequently the step change of T_c occurs; the temperature significantly drops. This sharp decrease is particularly evident in the case of nucleated samples. Finally (from 480 hrs), it decreases gradually again. The explanation of an increase of crystallization temperature at the beginning of irradiation (samples with 0.5 and 0.8 wt. % of nucleating agent) consists in the presumption that the decrease in molecular weight due to chain scission upon irradiation can increase the crystallization rate [48]. Nevertheless, the high concentration of defects contrariwise inhibits crystallization. Thus, at prolonged exposure time the T_c decreases. At the end of irradiation, the difference between T_c of neat and nucleated samples is lower than that at the beginning of irradiation (approx. 10 °C versus approx. 4 °C). It should be also noted that polypropylene with 0.2 wt. % of nucleating agent possesses earlier step drop of T_c as compared with the others (see Fig. 9.2.3).

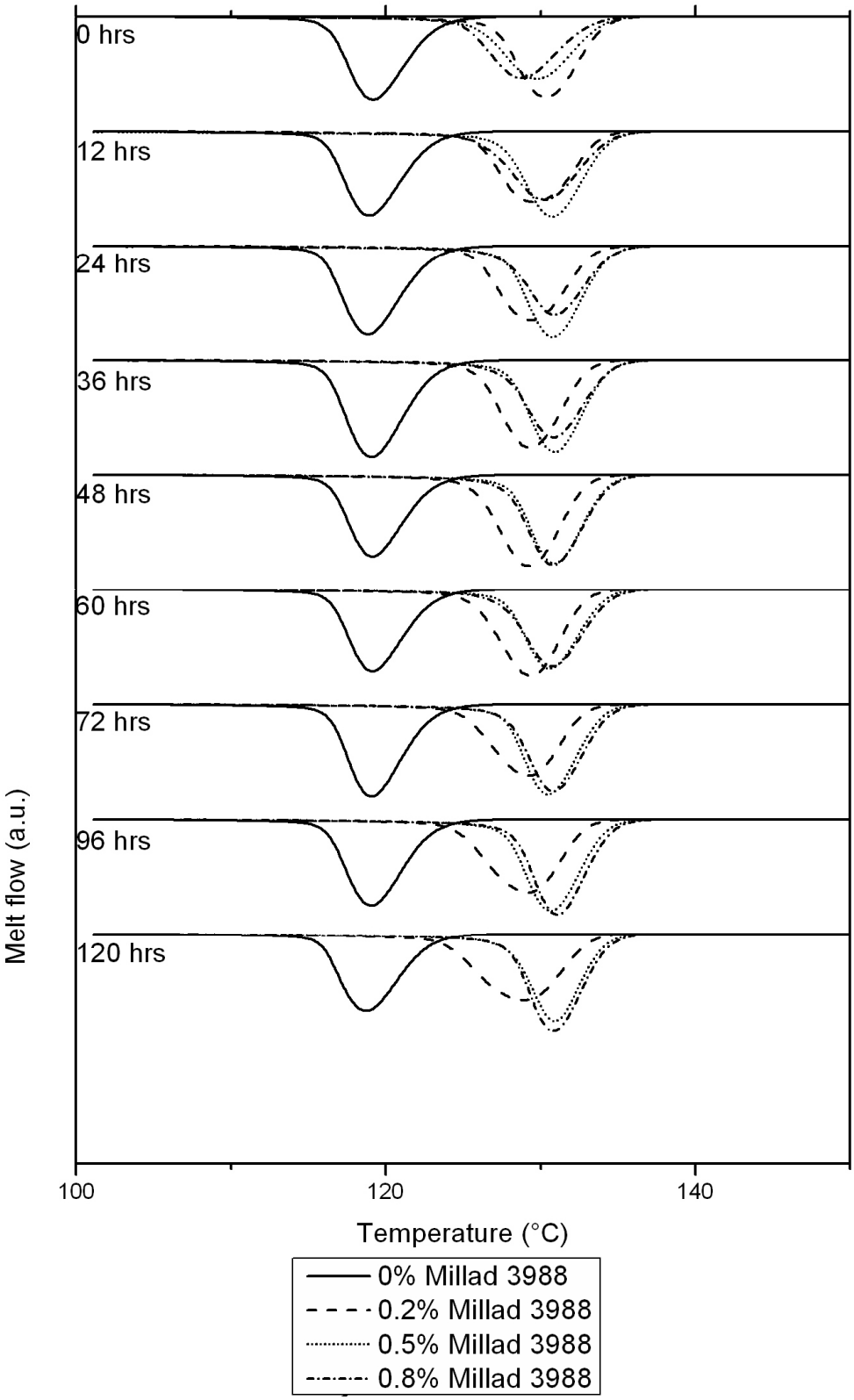

Fig. 9.2.1: Re-crystallization curves (0-120 hrs)

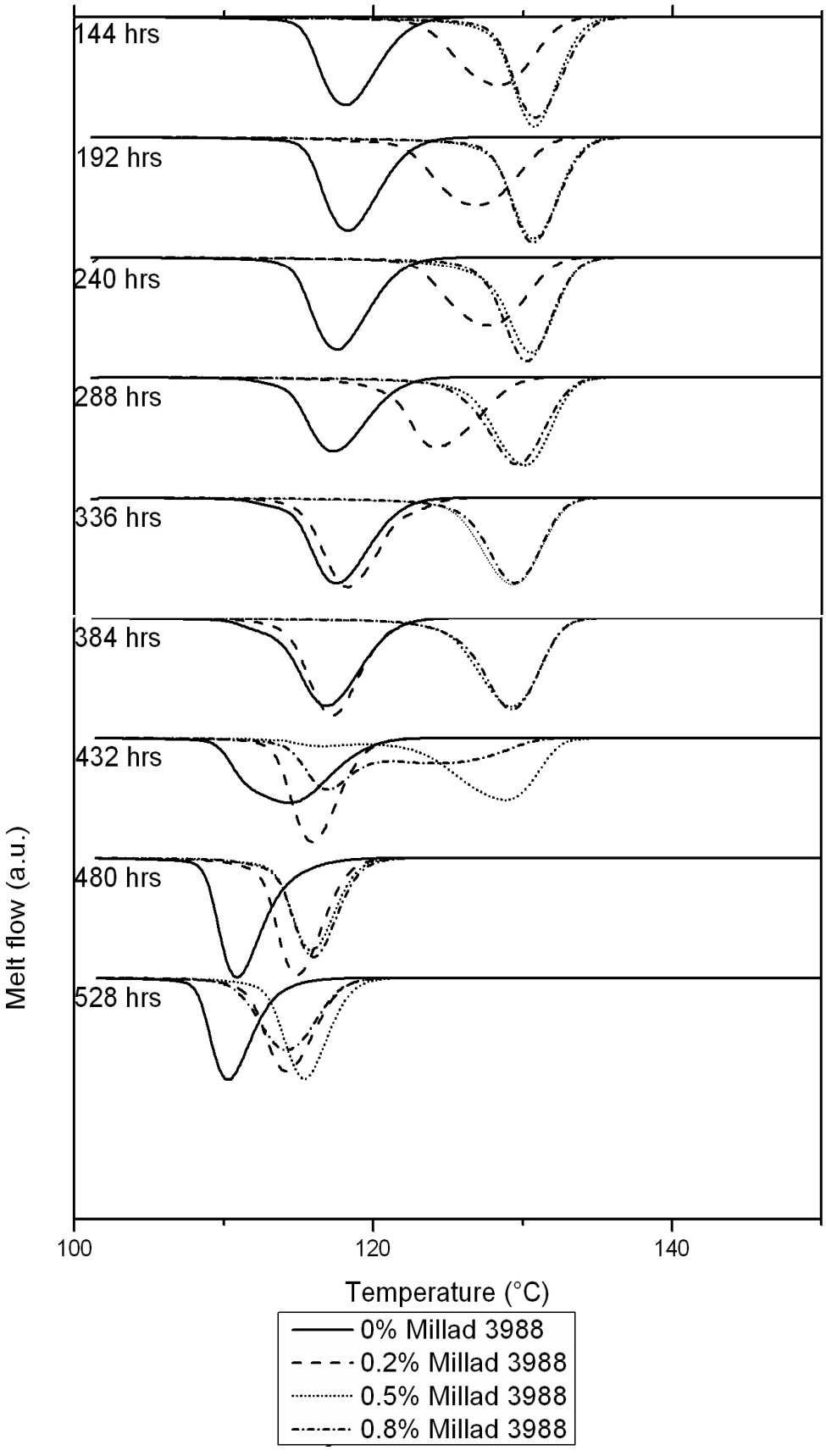

Fig. 9.2.2: Re-crystallization curves (144-528 hrs)

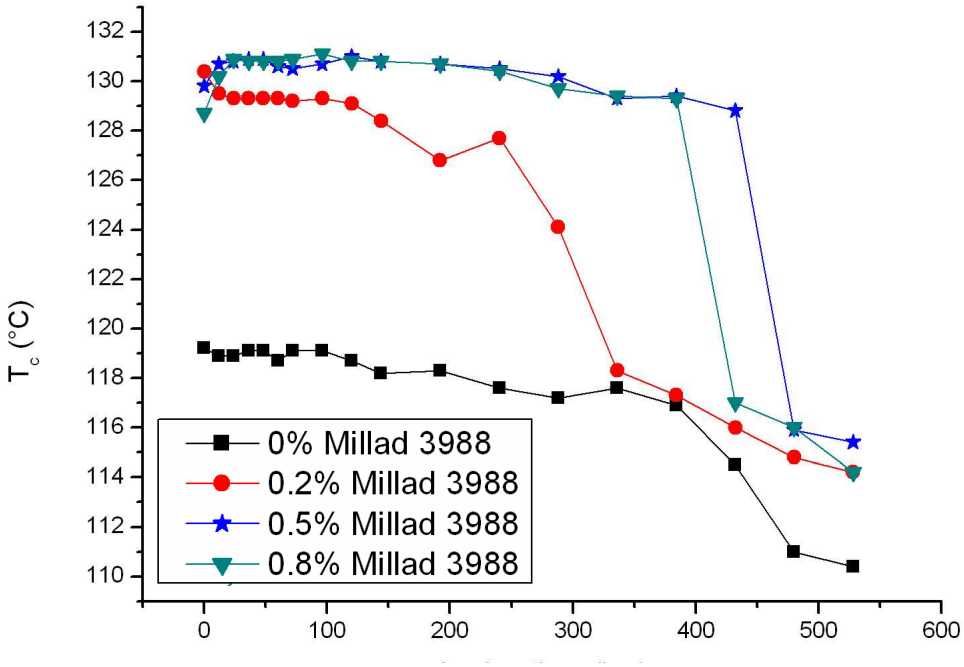

Fig. 9.2.3: The evolution of crystallization temperature during the irradiation

9.3 Re-melting

Non-isothermally crystallized samples were subsequently re-melted; corresponding thermograms are shown in Figs. 9.3.1 and 9.3.2. The general trend observed in all samples is the decrease of re-melting temperature (T_{m2}). T_{m2} of neat polypropylene is a bit lower than that of nucleated polypropylenes. Peaks of nucleated polypropylenes are practically identical. At higher exposure times, over 288 hours, all peaks become flat and splitted. The decrease of T_{m2} and broadening of endotherms are connected with incorporation of irregularities into the molecular chains. Such molecules form imperfect crystals with broad size distribution.

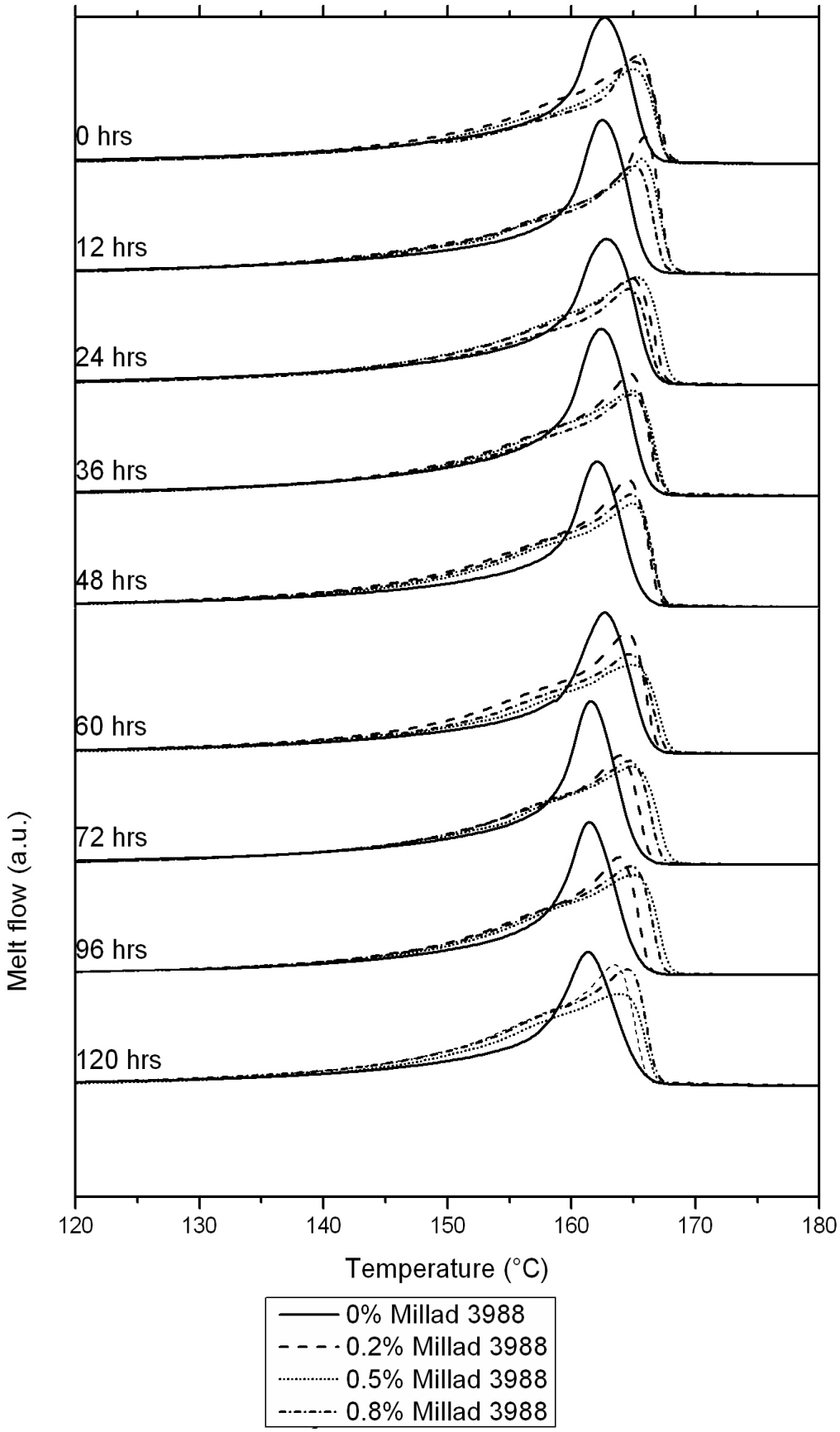

Fig. 9.3.1: Re-melting curves (0-120 hrs)

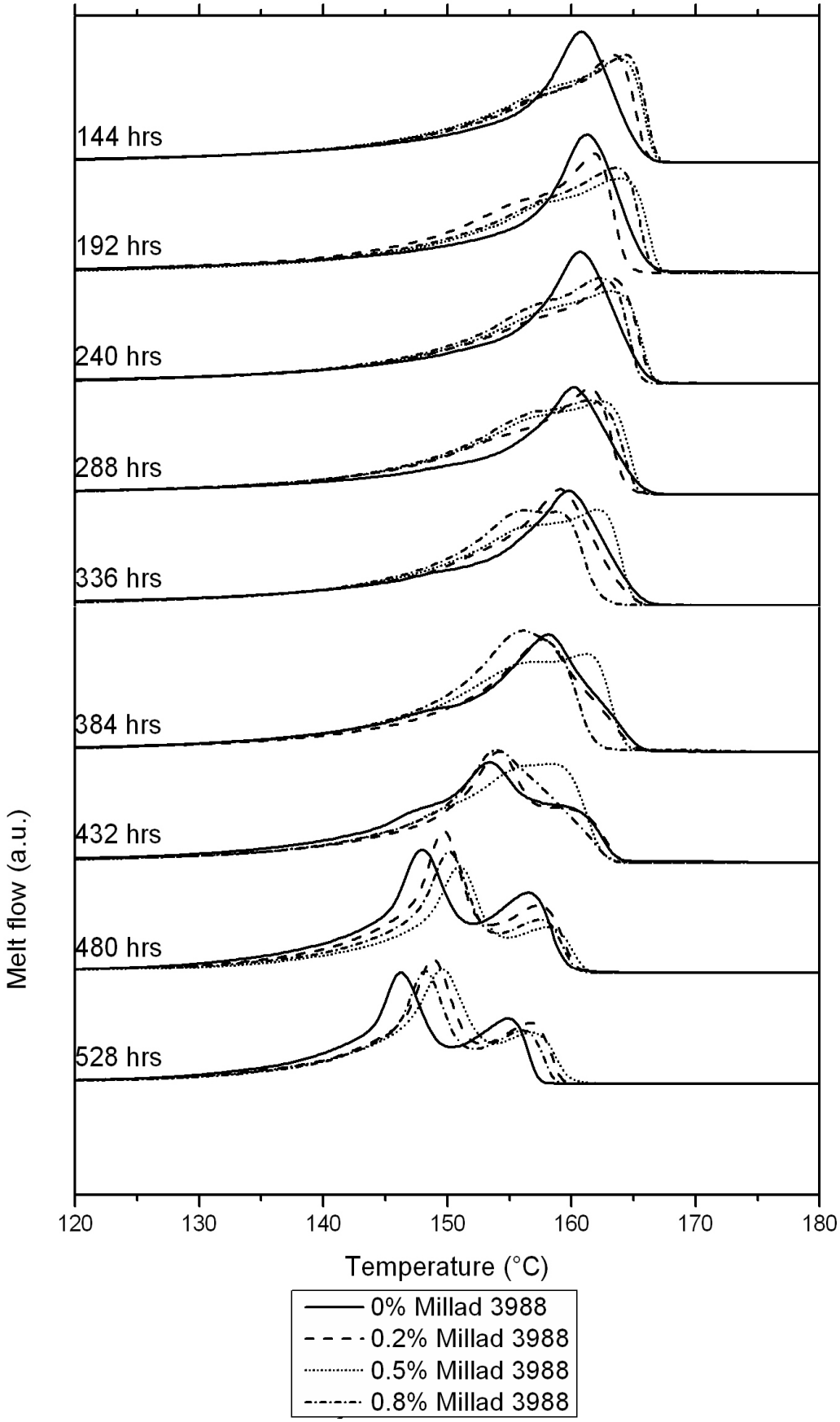

Fig. 9.3.2: Re-melting curves (144-528 hrs)

10 X-RAY DIFFRACTION

Wide-angle X-ray scattering was employed to observe the evolution of morphology upon UV-irradiation. The X-ray diffractograms of the UV-irradiated samples are shown in Figs. 10.1.1−10.1.4.

The diffractograms show the typical reflections for polypropylene at angles 2θ=14.2 °, 17 ° and 18.8 °. The diffractograms of each sample differ only in a proportion of individual peaks. It also slightly differs with UV-exposure. Nevertheless, no uniform or significant evolution of diffractograms is observed during irradiation.

From all diffractogram patterns the crystallinity was calculated (see Table 10.1). The evolution of crystallinity upon UV-exposure is plotted in Fig. 10.1.5. The results show that crystallinity strongly fluctuates with increasing irradiation time, nevertheless the general trend is slightly increasing crystallinity with increasing UV-exposure. This rise is connected with phenomenon called chemicrystallization; the scissions of molecular chains in the amorphous region release the molecular entanglements facilitating the additional crystallization in the solid state [48,49].

As can be seen in Fig. 10.1.5 the highest increase in crystallinity is observed for neat polypropylene. This can indicate its highest sensitivity to UV-irradiation.

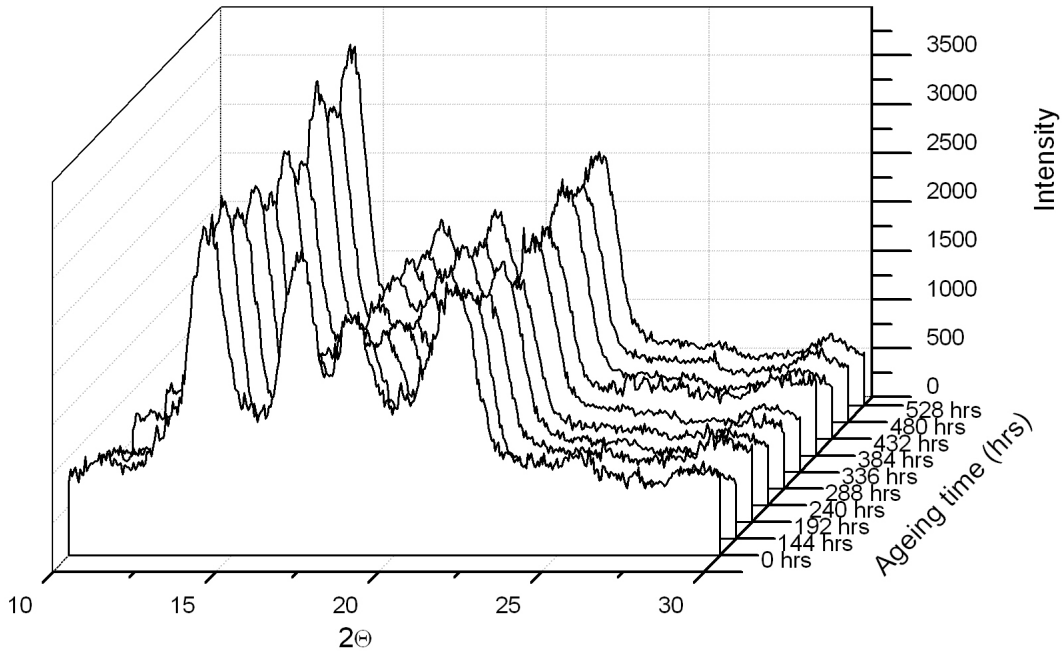

Fig. 10.1.1: The evolution of X-ray diffraction pattern with increasing exposure time for neat iPP

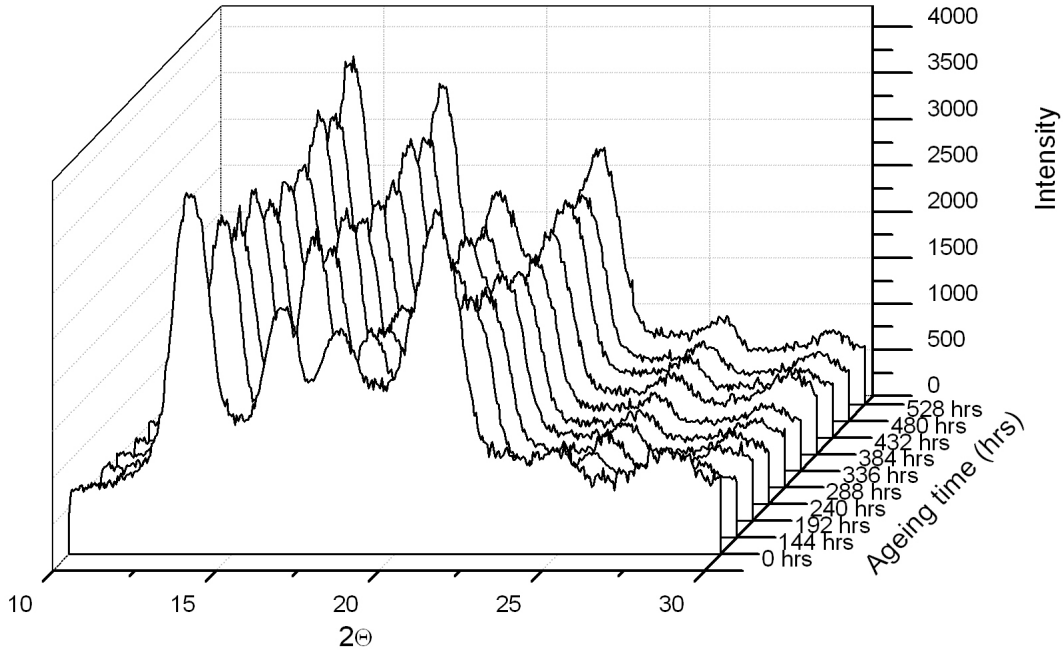

Fig. 10.1.2: The evolution of X-ray diffraction pattern with increasing exposure time for iPP + 0.2 % Millad 3988

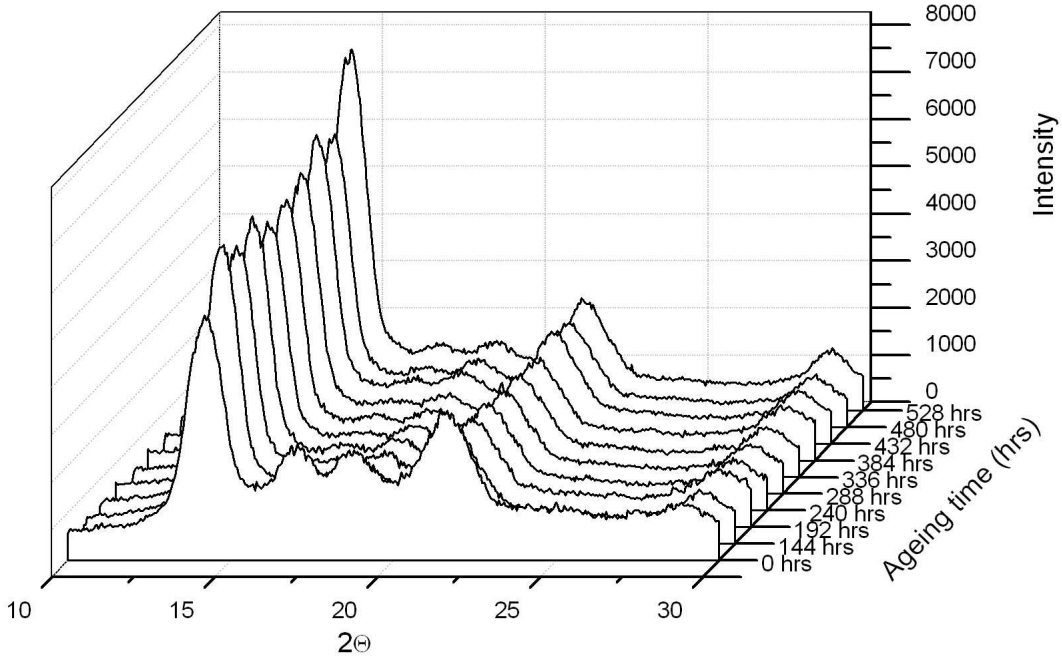

Fig. 10.1.3: The evolution of X-ray diffraction pattern with increasing exposure time for iPP + 0.5 % Millad 3988

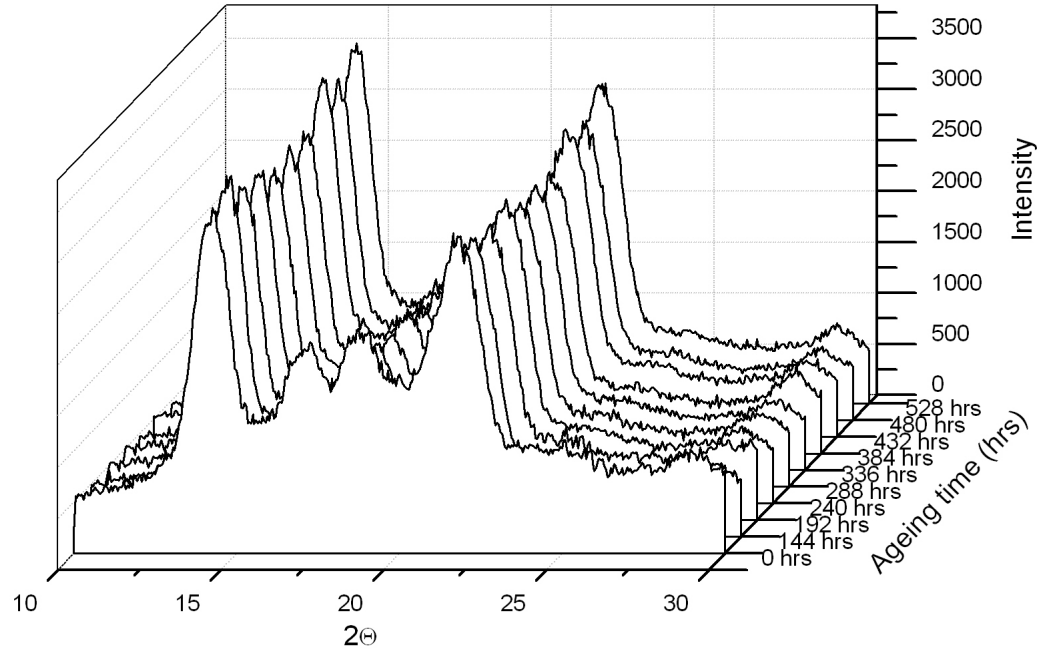

Fig. 10.1.4: The evolution of X-ray diffraction pattern with increasing exposure time for iPP + 0.8 % Millad 3988

Table 10.1: The evaluated data of X-ray measurement

Exposure time (hrs)	Crystallinity X_c			
	0% Millad 3988	0.2% Millad 3988	0.5% Millad 3988	0.8% Millad 3988
144	0.47	0.50	0.53	0.52
192	0.53	0.49	0.53	0.50
240	0.53	0.50	0.56	0.51
288	0.59	0.51	0.55	0.51
336	0.56	0.51	0.55	0.56
384	0.55	0.53	0.57	0.52
432	0.55	0.52	0.61	0.57
480	0.56	0.54	0.61	0.57
528	0.61	0.54	0.62	0.58

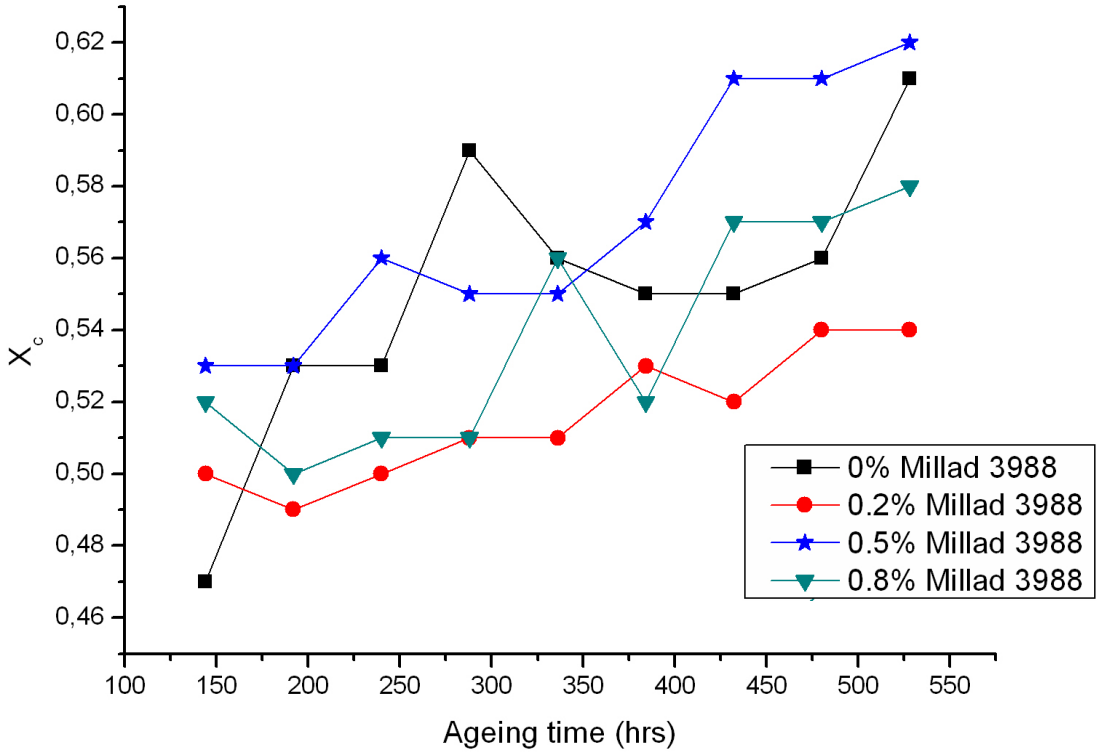

Fig. 10.1.5: The dependence of crystallinity on UV-exposure time

11 INFRARED SPECTROSCOPY

The results from infrared spectroscopy exhibit the growth of carbonyl groups expressed by carbonyl index with the exposure time for both neat and nucleated polypropylenes (Fig. 11.1.1). Shape of peaks is uniform for all studied samples.

In initiative time of exposure (0−150 hrs) carbonyl index values are zero. After this time period carbonyl index begin slightly increase. After this induction period (approx. 250 hours of UV-exposure) carbonyl index begins rapidly increase. This rapid growth starts quite earlier in the case of neat PP and PP with 0.8 wt. % of nucleating agent. Final values of carbonyl index of these samples are consequently about one point higher than that of polypropylene with 0.2 and 0.5 wt. % of nucleating agent.

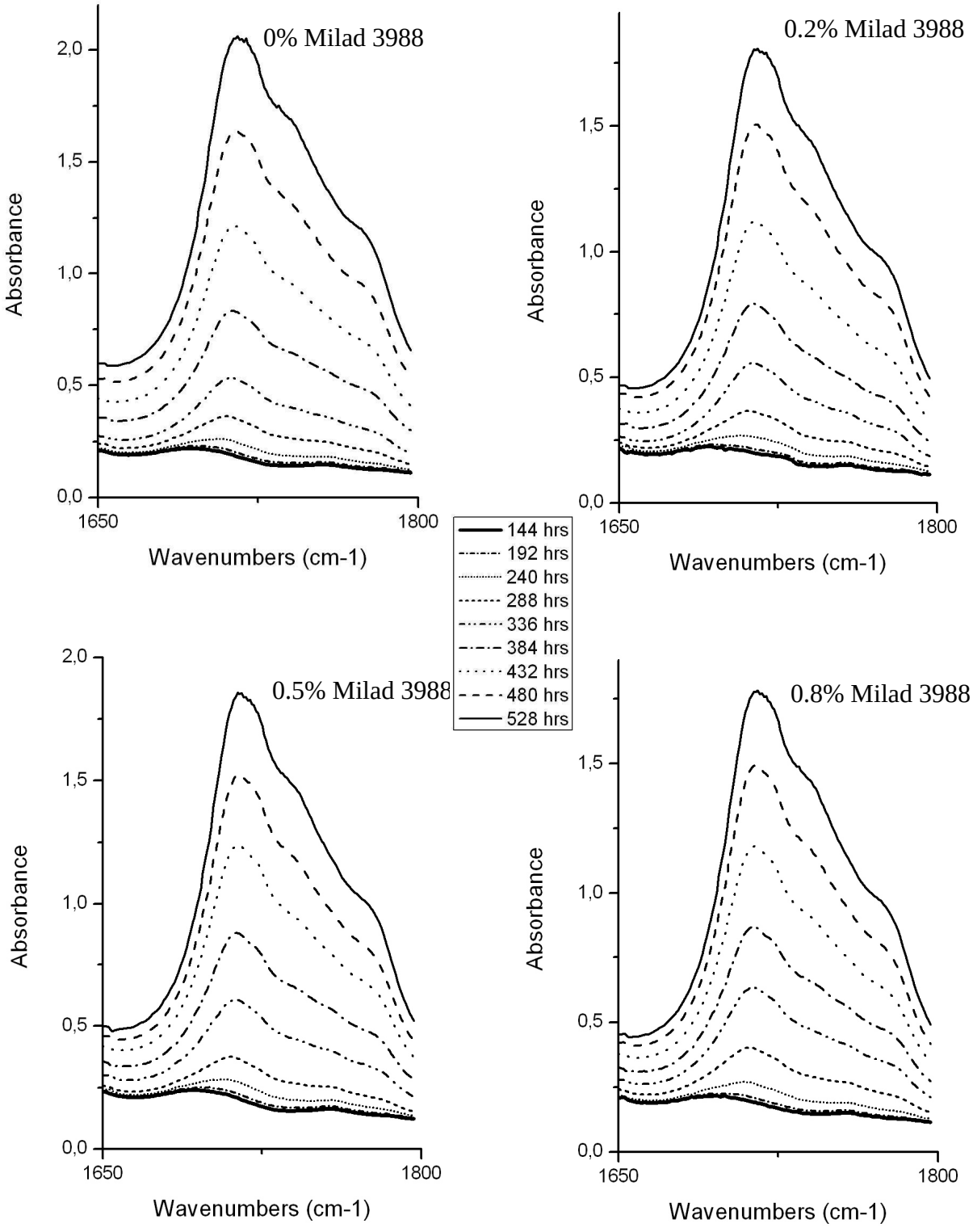

Fig. 11.1.1: FTIR changes of UV- irradiated samples

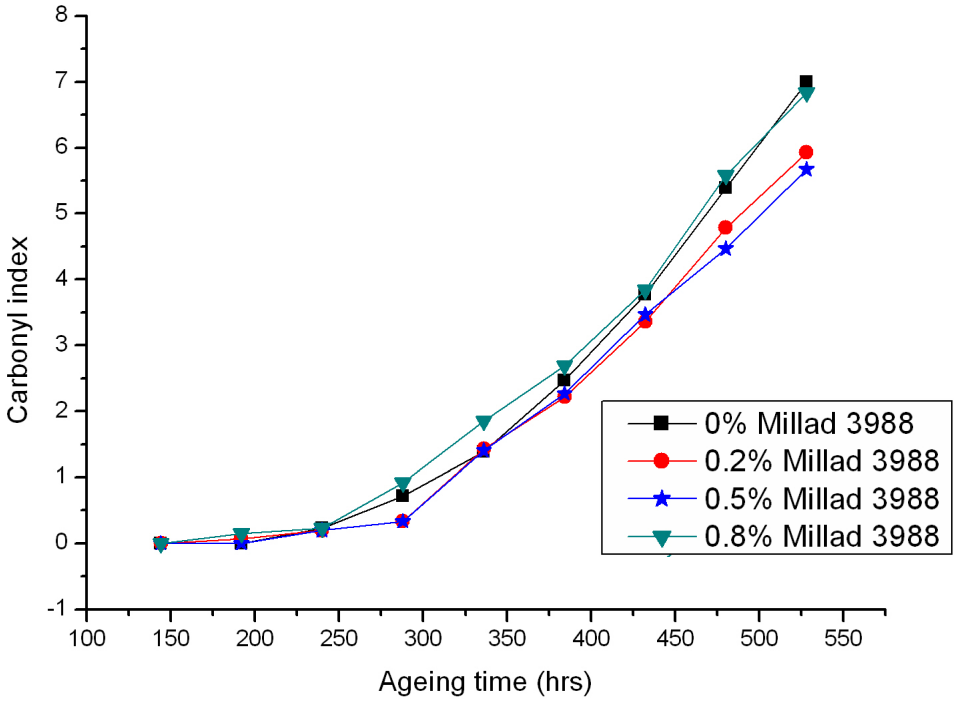

Fig. 11.1.2: Effect of UV-exposure on the carbonyl index of samples

12 OPTICAL STEREOMICROSCOPY

The micrographs from stereomicroscope display the surfaces of neat (Fig. 12.1.1) and nucleated (Figs. 12.1.2−12.1.4) polypropylenes. The evolution of cracks in dependence on irradiation time is observed. It can be seen that the difference between neat and nucleated samples is significant after longer time of UV-exposure.

The surface of all samples at the beginning of irradiation is smooth and there are not cracks or irregularities in evidence. Only fine structure, which is created by compression-moulding is observable. With increasing content of nucleating agent samples are a little more transparent.

After the irradiation time period about 288 hours the creation of cracks starts. With increasing time of exposure density of cracks also increases. The surface of UV-irradiated neat polypropylene shows dense network of cracks. With increasing time is this network more distinct, number of cracks is higher and they are also wider. The cracks of the nucleated samples are significantly different as compared to neat polypropylene. They extend in parallel lines. With increasing time the number of cracks is not significantly higher. As degradation proceeds wide and relatively short cracks associate to long splits which extend across the whole sample. This process is the same for all nucleated samples.

The difference of crack formation in neat and nucleated polypropylene is caused by different morphology. Actually, cracks in neat polypropylene copy the sperulite boundaries. However, in the case of nucleated material the crystals are too small, thus, different effect such as processing conditions plays a role in the formation of cracks.

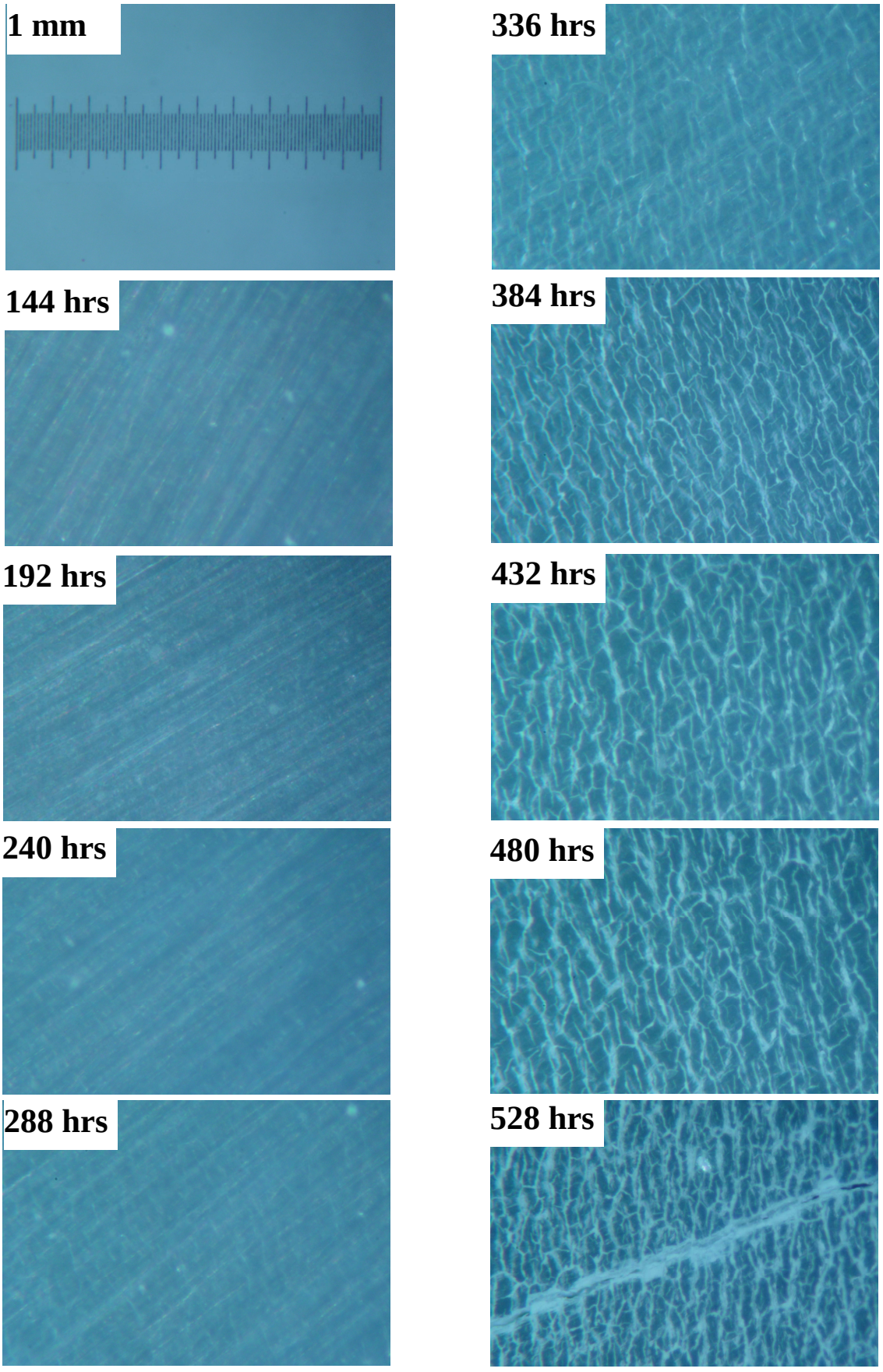

Fig. 12.1.1: Surfaces of neat polypropylene samples

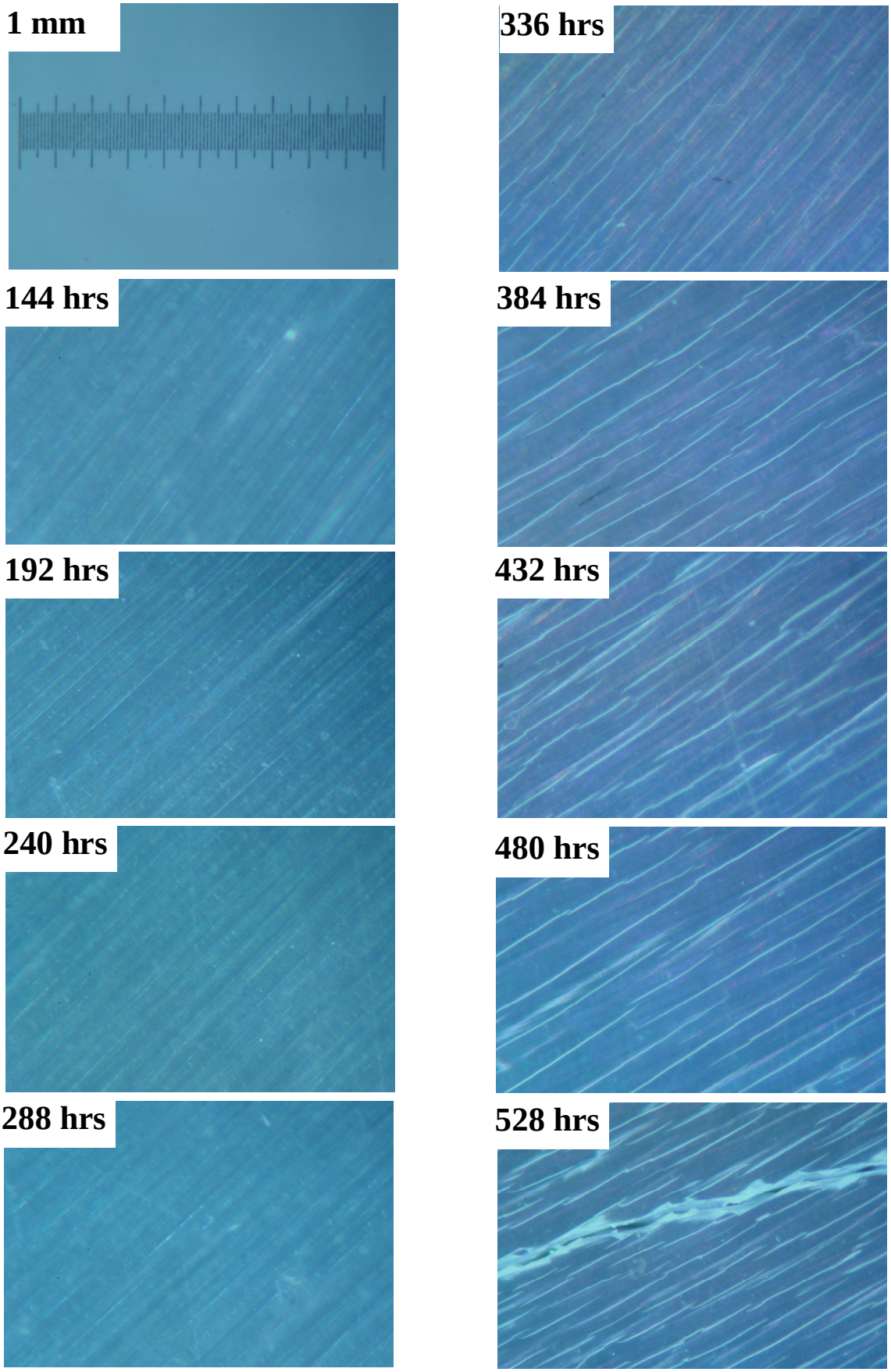

Fig. 12.1.2: Surfaces of polypropylene samples with content 0.2 % of nucleator

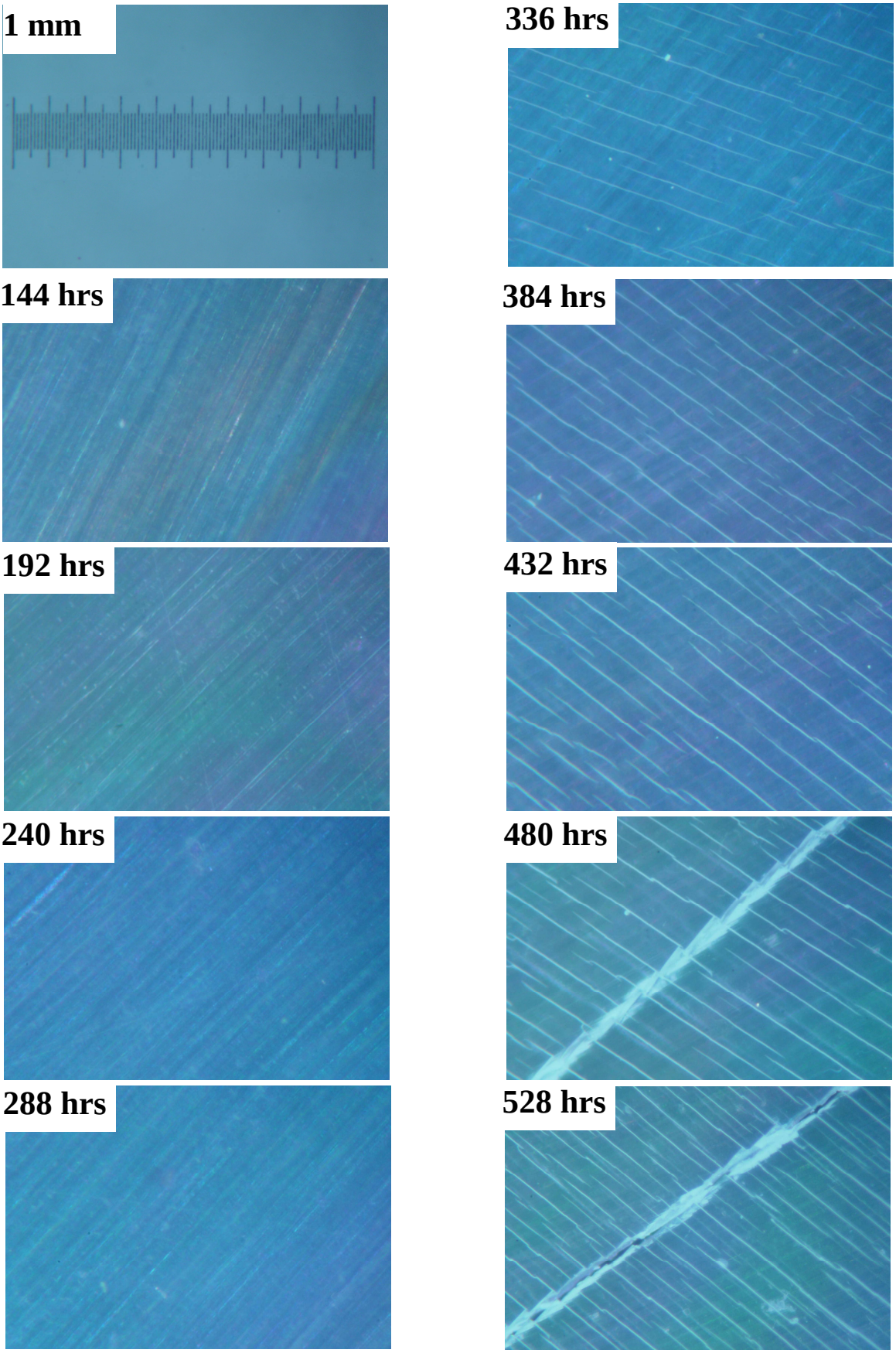

Fig. 12.1.3: Surfaces of polypropylene samples with content 0.5 % of nucleator

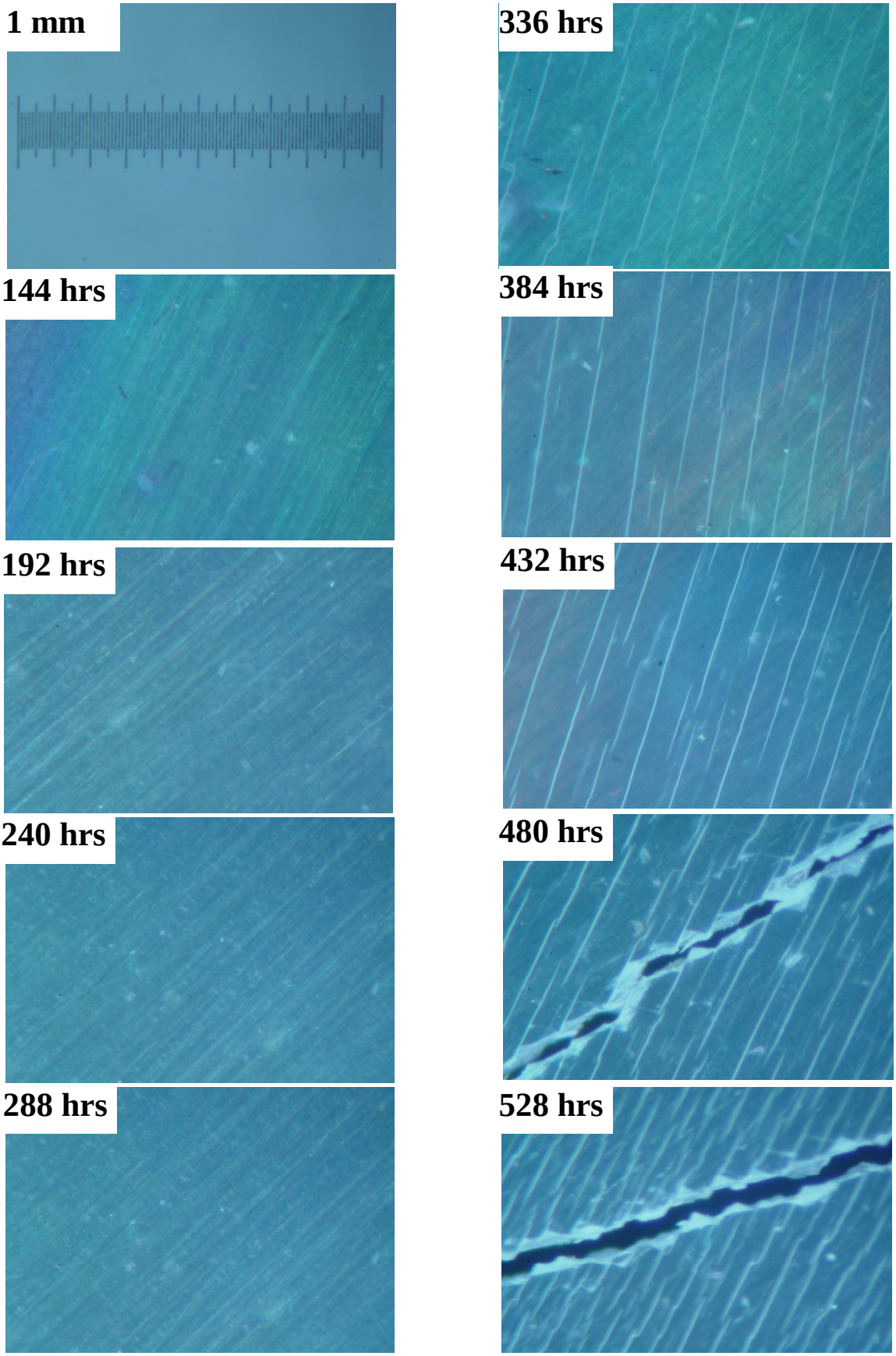

Fig. 12.1.4: Surfaces of polypropylene samples with content 0.8 % of nucleator

CONCLUSION

This Master thesis deals with the influence of α-nucleation on UV-degradation of isotactic polypropylene. Four different samples of polypropylene (neat PP and PP with content of 0.2, 0.5 and 0.8 wt. % of nucleator) were exposed to UV-irradiation and in various times were analyzed. For analyzing these samples methods like differential scanning calorimetry, X-ray diffraction, infrared spectroscopy and optical microscopy were used.

Differential scanning calorimetry measurement shows changes of melting and crystallization temperatures during irradiation. Melting temperature of all samples continuously decreases. This decrease is caused by erosion of the surfaces of the crystallites decreasing their thermodynamic stability. Re-crystallization temperature of neat polypropylene is significantly lower than that of nucleated polypropylenes due to the addition of heterogeneous nuclei into material which accelerates the crystallization. After long-term irradiation (approx. 240 hrs) step change of T_c occurs; the temperature significantly drops. Polypropylene with 0.2 wt. % of nucleating agent possesses the earliest step drop of T_c as compared with the others.

Results from X-ray diffraction indicate that crystallinity of all samples strongly fluctuates with increasing irradiation time, nevertheless the general trend is slight increase caused by chemicrystallization. The highest increase of crystallinity is observed for neat polypropylene. This can indicate its highest sensitivity to UV-irradiation.

Outcomes from infrared spectroscopy do not show any significant difference in growth of carbonyl groups neither neat nor nucleated polypropylene. Rapid growth of carbonyl index starts quite earlier in the case of neat PP and PP with 0.8 wt. % of nucleating agent. Final values of carbonyl index of these samples are consequently about one point higher than that of polypropylene with 0.2 and 0.5 wt. % of nucleating agent.

The stereomicroscope micrographs revealed the introduction of cracks on the surfaces during UV-exposure. Cracks of neat polypropylene create dense network on the boundaries of the spherulites whereas cracks of nucleated polypropylenes extend in parallel

lines. As the crystallites in these materials are very small the form and orientation of the cracks are probably influenced by the processing conditions during sample preparation.

Generally these results indicate that the presence of α-nucleating agent does not significantly influence the photooxidation of polypropylene. The changes in carbonyl index evolution are neglectable, as well as changes in melting temperature. Nevertheless the influence of nucleation on crystallization temperature and influence on appearance on surface of nucleated samples was discovered.

REFERENCES

[1] Nagasawa, S., Fujimori, A., Masuko, T., Iguchi, M. (2005) Polymer, 46, 5241

[2] Kristiansen, M., Gress, A., Smith, P., Hanft, D., Schmidt, H. W. (2006) Polymer, 47, 249

[3] Blomenhofer, M., Ganzleben, S., Hanft, D., Schmidt, H. W., Kristiansen, M., Smith, P., Stoll, K., Mader, D., Hoffmann, K. (2005) Macromolecules, 38, 3688

[4] Výchopňová, J. et al.: *The role of specific nucleation in polypropylene photodegradation*, Polymer Degradation and Stability 92 (2007) 1763-1768

[5] Gobi International: *Polypropylene – The International Market 2003* [online]. London (United Kingdom): Gobi International, 2003. Available on www.gobi.co.uk/pdfs/polypropylene.pdf.

[6] Mark S. M. Alger: *Polymer science dictionary*; New York; 1989

[7] Dostupné na WWW 1.4.2008: < www.eng.buffalo.edu>

[8] Brydson, J.: *Plastics Materials (7th Edition)*, Butterworth-Heinemann, 1999

[9] Monasse, B., Haudin, M. J.: *Polypropylene: Structure, blends and composites*, Vol. 1. Molecular structure of polypropylene homo- and copolymers, Chapman & Hall, London, 1995, ISBN 0-412-58430-1

[10] Maier, C., Calafut, T.: *Polypropylene - The Definitive User's Guide and Databook*, Norwich, Plastics Design Library, 1998, ISBN 1-884207-58-8

[11] Phillips, J. P., Mezghani, K.: *Polypropylene, Isotactic (Polymorphism)*, University of Tennessee, CRC Press, 1996, ISBN 0-8493-2470-X

[12] Dostupné na WWW 25.2.2008: <www.wrap.org.uk>

[13] Karger-Kocsis, J. *Polypropylene: An A-Z reference*. Dortrecht (Netherlands): Kluwer Academic Publishers, 1999, ISBN: 0-412-80200-7

[14] Kawai, T., Strobl, G.: *Crystallization Mechanism of sPP*, Physikalisches Institut Albert-Ludwigs-UniversitätFreiburg,Germany; (http://frsl06.physik.unifreiburg.de/docs/ks.pdf; 10.1.2005)

[15] Cheng, D. Z. S., Janimak, J. J., Rodrigues, J.: *Polypropylene: Structure, blends and composites*, Vol. 2. Crystalline structures of polypropylene homo- and copolymers, Chapman&Hall, London, 1995, ISBN 0-412-58430-1

[16] Turner-Jones, A., Aiylewood, J. M., Beckett, D. R.: (1964) *Jour. of Macromolecular Chem.*, Vol. 75, 134 – 154

[17] Salamone, J. C.: *Polymeric materials encyclopedia,* Boca Raton (United states of America): CRC Press, 1996.

[18] Varga, J.: *β-modification of isotactic polypropylene: preparation, structure, processing, properties, and application,* Journal of Macromolecular Science, 2002, No. 41, New York (United states of America): Marcel Dekker, 2002.

[19] Lezak, E., Bartzak, Z.: *Fibres and Textiles in Eastern Europe,* vol.13; No 5 (53); 2005

[20] Meille, S.V., Bruckner, S., Porzio, W.: γ*-isotactic polypropylene. A structure with nonparallel chain axes,* Macromolecules, 23, 4114-21, 1990

[21] Harper, Charles A.: *Modern Plastic Handbook,* Modern Plastic, Mc Graw-Hill, 2000, ISBN 978-0-07-026714-5

[22] Wypych, G.: *Handbook of Material Weathering (2nd Edition)*; ChemTec Publishing, 1995, ISBN: 1-895198-12-7

[23] Schnabel, W., *Polymer degradation*; Berlin: Akademie verlag 1981, ISBN: 1-56990-092-2

[24] Dostupné na WWW 17.5.2006: <http://gold.zvon.org/>

[25] Ranby,B., Rabek, J.F., *Photodegradation, photo-oxidation and photostabilization of polymers*; John Wiley & Sons Ltd., 1975, ISBN: 0-471-70788-0

[26] Chodák, I., *Crosslinking of polypropylene*; Polypropylene-An A-Z Reference; Kluwer Academic Publishers; 1999, ISBN: 0-412-80200-7

[27] Al-Malaika, S., *Photostabilizers*; Polypropylene-An A-Z Reference; Kluwer Academic Publishers; 1999, ISBN: 0-412-80200-7

[28] Obadal, M., Čermák, R., Raab, M., Verney, V., Commereuc, S., Fraisse, F., *Structure evolution of α- and β-polypropylenes upon UV irradiation: A multiscale comparison*; Polymer Degradation and Stability 88 (2005) 532-539

[29] Libster, D., Aserin, A., Garti, N., *Advanced nucleating agents for polypropylene*; Polymers for Advanced Technologies, 18 (2007) 685-695

[30] Shan, V., *Handbook of Plastics Testing Technology, 2nd ed.*, A Wiley-Interscience publication, USA, 1998. ISBN 0-471-18202-8.

[31] Dostupné na WWW 9.4.2008: < http://www.cnep-ubp.com/>

[32] Dean, John A., *The Analytical Chemistry Handbook*, New York. McGraw Hill, pp. 15.1–15.5, 1995

[33] Pungor, E., *A Practical Guide to Instrumental Analysis*, Boca Raton, Florida, 1995. pp. 181–191.

[34] Skoog, Douglas A., Holler, J., Nieman, T., *Principles of Instrumental Analysis*. Fith Edition. New York; pp. 905–908; 1998

[35] Dostupné na WWW 9.4.2008: < http://evitherm.athena.as/>

[36] Cheremisinoff, N. P., *Polymer Characterization – Laboratory Techniques and Analysis*, Notes Publications in 1996, ISBN 0-8155-1403-4

[37] Brundle, C. R., Evans, Charles A. Jr., Wilson, S., *Encyclopedia of Materials Characterization - Surfaces, Interfaces, Thin Films*, Elsevier, 1992, ISBN 978-0-7506-9168-0

[38] Campbell, D., White, J. R., *Polymer Characterization Physical Techniques*, London, 1989

[39] Tissue, Brian M.,; *X-ray Diffraction*; 2000; (http://elchem.kaist.ac.kr/vt/chem-ed/diffract/xray.htm; 1.5.2007)

[40] Guest Article by Sampath S. Iyengar; *Analysis of Materials by X-Ray Diffraction*; Technology of Materials - 909.471.8194

[41] Dostupné na WWW 10.4.2008: <http://en.wikipedia.org/wiki/Infrared_spectroscopy>

[42] Dostupné na WWW 10.4.2008: <http://lms.vscht.cz/Zverze/Infrared.htm>

[43] Dostupné na WWW 10.4.2008: <http://scienceofspectroscopy.info/edit/index.php?title=Infrared_Spectroscopy>

[44] Dostupné na WWW 10.4.2008: <http://en.wikipedia.org/wiki/Fourier_transform_spectroscopy>

[45] Dostupné na WWW 10.4.2008: http://solidstate.physics.sunysb.edu/

[46] Dostupné na WWW 10.4.2008: http://www.nikoninstruments.com

[47] Dostupné na WWW 10.4.2008: <http://www.microscopyu.com>

[48] Rabello, M. S., White, J. R., *The role of physical structure and morphology in the photodegradation behaviour of polypropylene*; Polym. Deg. Stab., 1997, 56, 57-73

[49] Rabello, M. S., White, J. R., *Crystallization and melting behaviour of photodegraded polypropylene*; Polymer, 1997, 38(26), 6389-6399

REVIEW OF SYMBOLS

PP	Polypropylene
iPP	Isotactic polypropylene
sPP	Syndiotactic polypropylene
aPP	Atactic polypropylene
T_c	Crystallization temperature (°C)
T_{m1}	Melting temperature (°C)
T_{m2}	Re-melting temperature (°C)
T_g	Glas transition temperature (°C)
α	Monoclinic crystalline form
β	Trigonal crystalline form
γ	Orthorhombic crystalline form
α_I	Positive birefringence spherulites
α_{II}	Negative birefringence spherulites
α_{III}	Mixed birefringence spherulites
a, b, c	Signification of lengths (nm)
ρ	Density (kg/m^3)
M_n	Number-average molecular weight (g/mol)
M_w	Weight-average molecular weight (g/mol)
DBS	1,2,3,4-bis-dibenzylidene sorbitol
DOS	1,2,3,4-bis-(*p*-methoxybenzylidene) sorbitol
MDBS	1,2,3,4-bis-(*p*-methylbenzylidene) sorbitol
DMDBS	1,2,3,4-bis-(3,4-dimethylbenzylidene) sorbitol
UV	Ultraviolet
E	Energy of radiation (J)
ν	Frequency of radiation (1/s)
h	Planck's constant (J.s)
S_0	Ground state of molecules
DSC	Differential scanning calorimetry
DTA	Differential thermal analysis
XRD	X-ray diffraction
θ	Angle of X-ray diffraction

n	Integer
λ	Wavelnegth (nm)
IR	Infrared
FTIR	Fourier-transform infrared
GFP	Fluorescence illumination
WAXS	Wide angle X-ray scattering
X_c	Crystallinity
ΔH_{m1}	Melting enthalpy (J/g)
ΔH_c	Crystallization enthalpy (J/g)
ΔH_{m2}	Re-melting enthalpy (J/g)

REVIEW OF FIGURES

REVIEW OF TABLES

REVIEW OF EQUATIONS

APPENDICES

Appendice Nr. 1: Crystallization and melting characteristic of samples obtained by DSC

Irradiation time (h)	Sample (% of Millad 3988)	T_{m1} (℃)		ΔH_{m1} (J/g)	T_c (℃)	ΔH_c (J/g)	T_{m2} (℃)		ΔH_{m2} (J/g)
		α1	α2				α1	α2	
0	0 %	164.1		93	119.2	-101	162.8		102
	0.2 %	163.3		101	130.4	-103	165.2		109
	0.5 %	161.9		86	129.8	-92	164.9		91
	0.8 %	162.2		84	128.7	-90	165.4		87
12	0 %	164.0		91	118.9	-102	162.5		91
	0.2 %	163.4		103	129.5	-107	165.9		111
	0.5 %	163.3		106	130.7	-109	165.6		112
	0.8 %	162.3		113	130.2	-103	165.0		109
24	0 %	164.4		106	118.9	-110	162.9		111
	0.2 %	163.0		103	129.3	-104	164.8		112
	0.5 %	162.3		112	130.8	-114	165.2		123
	0.8 %	161.7		93	130.9	-89	164.6		98
36	0 %	163.5		117	119.1	-120	162.4		121
	0.2 %	163.1		111	129.3	-113	164.7		118
	0.5 %	161.8		102	130.9	-108	164.9		113
	0.8 %	162.0		85	130.8	-98	164.9		93
48	0 %	163.7		98	119.1	-96	162.1		94
	0.2 %	163.1		112	129.3	-118	164.5		112
	0.5 %	162.0		96	130.9	-103	164.9		99
	0.8 %	162.2		107	130.8	-108	164.7		111
60	0 %	164.3		92	118.7	-98	162.5		93
	0.2 %	163.0		115	129.3	-111	164.5		114
	0.5 %	162.1		89	130.6	-93	164.9		93
	0.8 %	162.4		95	130.8	-99	164.7		101
72	0 %	164.2		102	119.1	-106	161.7		101
	0.2 %	162.7		94	129.2	-99	164.1		97
	0.5 %	162.2		97	130.5	-104	165.0		103
	0.8 %	162.3		96	130.9	-105	164.7		101
96	0 %	164.0		98	119.1	-101	161.4		101
	0.2 %	163.0		106	129.3	-109	163.9		109
	0.5 %	162.3		103	130.7	-108	165.1		107
	0.8 %	162.4		106	131.1	-110	164.8		111
120	0 %	164.6		92	118.7	-94	161.5		92
	0.2 %	163.0		108	129.1	-113	163.5		110
	0.5 %	161.7		93	131.0	-100	164.1		97
	0.8 %	162.1		109	130.8	-114	164.6		111
144	0 %	163.9		96	118.2	-103	160.9		98
	0.2 %	163.1		103	128.4	-107	163.3		103
	0.5 %	162.2		107	130.8	-120	164.0		116
	0.8 %	161.8		103	130.8	-107	164.3		106
192	0 %	164.0		103	118.3	-108	161.3		101
	0.2 %	162.7		108	126.8	-112	161.8		108
	0.5 %	162.3		110	130.7	-107	164.0		105
	0.8 %	161.8		107	130.7	-110	163.5		107

Irradiation time (h)	Sample (% of Millad 3988)	T_{m1} (℃)		ΔH_{m1} (J/g)	T_c (℃)	ΔH_c (J/g)	T_{m2} (℃)		ΔH_{m2} (J/g)
		α1	α2				α1	α2	
240	0 %	163.9		114	117.6	-110	160.8		112
	0.2 %	163.5		105	127.7	-107	163.3		105
	0.5 %	162.3		100	130.5	-108	163.3		109
	0.8 %	162.0		107	130.4	-112	162.5		112
288	0 %	163.9		84	117.2	-93	160.2		88
	0.2 %	162.9		99	124.1	-102	161.6		100
	0.5 %	161.3		104	130.2	-109	162.5		110
	0.8 %	161.3		98	129.7	-104	161.8		105
336	0 %	163.4		99	117.6	-106	159.7		105
	0.2 %	162.2		107	118.3	-108	159.2		104
	0.5 %	161.4		105	129.3	-111	162.2		109
	0.8 %	159.7		101	129.4	-100	156.2		102
384	0 %	158.9		116	116.9	-118	158.1		114
	0.2 %	162.0		114	117.3	-110	157.8		102
	0.5 %	161.0		109	129.4	-118	161.1		113
	0.8 %	155.4	159.2	114	129.3	-114	156.1		111
432	0 %	156.3	159.9	109	114.5	-112	153.4		103
	0.2 %	153.8	160.6	105	116.0	-104	154.3		94
	0.5 %	158.0	161.2	108	128.8	-110	158.7		108
	0.8 %	158.5		109	117.0	-110	154.0		101
480	0 %	153.2		131	111.0	-117	148.0	156.8	110
	0.2 %	154.4	157.1	129	114.8	-114	149.9	157.6	105
	0.5 %	152.3	157.0	97	115.9	-87	151.0	158.1	81
	0.8 %	153.4	157.2	108	116.0	-96	150.2	157.6	90
528	0 %	152.7		107	110.4	-91	146.4	155.1	88
	0.2 %	152.8	156.4	116	114.2	-98	149.1	157.2	92
	0.5 %	152.3	156.8	111	115.4	-96	149.8	157.0	92
	0.8 %	153.1	156.5	100	114.2	-85	148.1	156.2	81